Manuscript Details

Manuscript number	ENGSTRUCT_2018_4107_R1
Title	UNCERTAINTIES IN DYNAMIC RESPONSE OF BUILDINGS WITH NON-LINEAR BASE-ISOLATORS
Article type	Research Paper

Abstract

Dynamic response of base-isolated buildings under uni-directional sinusoidal base excitation is numerically investigated considering uncertainties in the isolation and excitation parameters. The buildings are idealized as single degree of freedom (SDOF) system and multi-degrees of freedom (MDOF) system with one lateral degree of freedom at each floor level. The isolation system is modeled using two different mathematical models such as: (i) code-recommended equivalent linear elastic-viscous damping model and (ii) bi-linear hysteretic model. The uncertain parameters of the isolator considered are time period, damping ratio, and yield displacement. Moreover, the amplitude and frequency of the sinusoidal base excitation function are considered uncertain. The uncertainty propagation is investigated using generalized polynomial chaos (gPC) expansion technique. The unknown gPC expansion coefficients are obtained by non-intrusive sparse grid collocation scheme. Efficiency of the technique is compared with the sampling method of Monte Carlo (MC) simulation. The stochastic response quantities of interest considered are bearing displacement and top floor acceleration of the building. Effects of individual uncertain parameters on the building response are quantified using sensitivity analyses. Effect of various uncertainty levels of the input parameters on the dynamic response of the building is also investigated. The peak bearing displacement and top floor acceleration are more influenced by the amplitude and frequency of the sinusoidal base excitation function. The effective time period of the isolation system also produces a considerable influence. However, in the presence of similar uncertainty level in the time period, amplitude and frequency of the sinusoidal forcing function, the effect of uncertainties in the other parameters of the isolator (e.g., damping ratio and yield displacement) is comparatively less. Interestingly, the mean values of the response quantities are found to be higher than the deterministic values in several instances, indicating the need of conducting stochastic analysis. The gPC expansion technique presented here is found to be a computationally efficient yet accurate alternative to the MC simulation for numerically modeling the uncertainty propagation in the dynamic response analyses of the base-isolated buildings.

Keywords	Base isolation; bi-linear; equivalent linear; generalized polynomial chaos; hysteresis; non-intrusive; sensitivity; stochastic; sparse grid collocation; uncertainty
Taxonomy	Passive Control of Structure, Earthquake Engineering, Structural Dynamics, Passive Seismic Isolation, Probability-Based Design of Structures, Vibration Isolation
Manuscript region of origin	Europe

Corresponding Author	Vasant Matsagar
Corresponding Author's Institution	Indian Institute of Technology (IIT) Delhi
Order of Authors	Anoop Kodakkal, Sandip Kumar Saha, Kheirollah Sepahvand, Vasant Matsagar, Fabian Duddeck, Steffen Marburg
Suggested reviewers	Cenk Alhan, Henri Gavin, Goodarz Ahmadi

UNCERTAINTIES IN DYNAMIC RESPONSE OF BUILDINGS WITH NON-LINEAR BASE-ISOLATORS

Anoop Kodakkal[1,a], Sandip K. Saha[2,b], Kheirollah Sepahvand[3,a], Vasant A. Matsagar[4,a,c], Fabian Duddeck[5,a,d], and Steffen Marburg[6,a]

[a] *Technische Universität München* (*TUM*), *Germany*.
[b] *Indian Institute of Technology* (*IIT*) *Mandi*, *India*.
[c] *Indian Institute of Technology* (*IIT*) *Delhi*, *India*.
[d] *Queen Mary University of London* (*QMUL*), *UK*.

ABSTRACT

Dynamic response of base-isolated buildings under uni-directional sinusoidal base excitation is numerically investigated considering uncertainties in the isolation and excitation parameters. The buildings are idealized as single degree of freedom (SDOF) system and multi-degrees of freedom (MDOF) system with one lateral degree of freedom at each floor level. The isolation system is modeled using two different mathematical models such as: (i) code-recommended equivalent linear elastic-viscous damping model and (ii) bi-linear hysteretic model. The uncertain parameters of the isolator considered are time period, damping ratio, and yield displacement. Moreover, the amplitude and frequency of the sinusoidal base excitation function are considered uncertain. The uncertainty propagation is investigated using generalized polynomial chaos (gPC) expansion technique. The unknown gPC expansion coefficients are obtained by non-intrusive sparse grid collocation scheme. Efficiency of the technique is compared with the sampling method of Monte Carlo (MC) simulation. The stochastic response quantities of interest considered are bearing displacement and top floor acceleration of the building. Effects of individual uncertain parameters on the building response are quantified

[1] Graduate Student, E-Mail: anoop.kodakkal@tum.de
[2] Assistant Professor, E-Mail: sandip_saha@iitmandi.ac.in
[3] Senior Lecturer, E-Mail: k.sepahvand@tum.de
[4] Dogra Chair Professor, Humboldt Research Fellow, matsagar@civil.iitd.ac.in; Communicating Author, E-Mail: vasant.matsagar@tum.de
[5] Professor, E-Mail: duddeck@tum.de; f.duddeck@qmul.ac.uk
[6] Professor, E-Mail: steffen.marburg@tum.de

using sensitivity analyses. Effect of various uncertainty levels of the input parameters on the dynamic response of the building is also investigated. The peak bearing displacement and top floor acceleration are more influenced by the amplitude and frequency of the sinusoidal base excitation function. The effective time period of the isolation system also produces a considerable influence. However, in the presence of similar uncertainty level in the time period, amplitude and frequency of the sinusoidal forcing function, the effect of uncertainties in the other parameters of the isolator (e.g., damping ratio and yield displacement) is comparatively less. Interestingly, the mean values of the response quantities are found to be higher than the deterministic values in several instances, indicating the need of conducting stochastic analysis. The gPC expansion technique presented here is found to be a computationally efficient yet accurate alternative to the MC simulation for numerically modeling the uncertainty propagation in the dynamic response analyses of the base-isolated buildings.

Keywords: Base isolation; bi-linear; equivalent linear; generalized polynomial chaos; hysteresis; non-intrusive; sensitivity; stochastic; sparse grid collocation; uncertainty.

1. INTRODUCTION

Use of base isolation technique to protect buildings and other components from earthquake ground shaking is well-established (Kelly 1986, Buckle and Mayes 1990, Jangid and Datta 1995a, Warn and Ryan 2012). In practice, deterministic approach is adopted for analysis and design of the base-isolated structures. However, in reality, the characteristic/ mechanical model parameters of the isolation systems are uncertain. Therefore, stochastic analysis is essential for the accurate assessment of the performance of a base-isolated structure. In the stochastic approach, each variable is considered random and the associated uncertainty is represented by a probabilistic measure such as a probability density function (PDF). Schuëller and Pradlwarter

(2009) presented a detailed review of various sampling and non-sampling approaches of the stochastic analysis used for structural systems having uncertain input parameters.

Matsagar and Jangid (2004) presented a deterministic study, signifying the influence of the isolator parameters on the seismic response of the base-isolated buildings. The responses were compared for two isolator models; namely, equivalent linear elastic-viscous damping behavior and bi-linear hysteretic behavior. The results suggested that shape of the isolator hysteresis loop has significant influence on the seismic response of the base-isolated buildings. Lately, Amadio et al. (2016) also reported that the approach of equivalent linearization of the non-linear force-deformation behavior of a structure significantly affects the seismic response. However, they considered variation of the isolation parameters through deterministic approach. Therefore, it will be interesting to investigate the influence of isolator parameters on the seismic response of the base-isolated structures considering uncertainties in the isolator and excitation parameters.

In most of the earlier studies on stochastic analysis of the base-isolated structures, only the excitation function parameters were considered uncertain (Ahmadi 1983, Jangid and Datta1995b, Jangid 2000). Later, Li and Chen (2004) considered uncertainties in both the system parameters and the excitation function parameters. The stochastic response of the structure was determined using Monte Carlo (MC) simulations. Alhan and Gavin (2005) presented reliability analysis of a four-story base-isolated structure considering uncertainties in the isolation system characteristics. In their study, uncertainty of the isolator and ground motion characteristics were included. The MC simulation was used to determine the PDF of responses and the probability of failure. Jacob et al. (2013) considered uncertainty in the characteristics of the earthquakes and analyzed stochastic response of base-isolated buildings. Greco et al. (2016) presented robust design optimization of base isolation system with linear behavior wherein the structure was modeled by a linear single degree of freedom system. Markou et al.

(2018 and 2019) considered the uncertainty of the hybrid isolation parameters and employed the MC simulation to compute the stochastic response. The superstructure was modeled as a shear beam type, multi-degree of freedom model with four degrees of freedom.

It is observed that computationally involved sampling methods, such as the MC simulation, were used in majority of the earlier studies. The accuracy of the MC simulation largely depends on the number of realizations used. The structural model is analyzed for a large set of input parameters to achieve the desired accuracy level. This process results in enormous processing time leading to significantly increased computational costs. Therefore, it is necessary to explore for a computationally efficient numerical procedure for stochastic analysis of the base-isolated structures.

Generalized polynomial chaos (gPC) expansion technique has received considerable attention in engineering applications in the recent years. Wiener (1938) introduced this numerical technique in early 20th century as a homogeneous chaos method. The use of this technique in engineering problems was rare until last decade (Xiu and Karniadakis 2002). The gPC expansion technique approximates both the input and output parameters by truncated orthogonal polynomial series. Sepahvand et al. (2010) presented a detailed description of the gPC expansion technique and explained its application in vibro-acoustic problems. Saha et al. (2013) presented a step-by-step numerical procedure for dynamic response analysis of the base-isolated liquid storage tanks, considering uncertain isolation and excitation parameters, using the gPC expansion-based simulation technique in time domain. However, non-linearity in the isolation system was not considered in their studies, which has been concluded to have significant influence on the response of the base-isolated structures (Matsagar and Jangid 2004). Therefore, a numerical modeling technique is required to be developed for dynamic analysis of structures with non-linear base isolators considering uncertainties in the model parameters.

Herein, the stochastic responses of the base-isolated buildings are evaluated using the gPC expansion technique considering uncertain isolator and excitation function parameters. To avoid the large computational efforts, a non-sampling technique is adopted for the present study based on the gPC expansion. Computational efficiency of the adopted technique is also compared with that of the MC simulation to represent the stochasticity of the response of the base-isolated buildings. Influence of the uncertain isolation and excitation parameters on the peak response of the base-isolated buildings is investigated, when the isolation system is modeled using the code-recommended equivalent linear elastic-viscous damping model and bi-linear hysteretic model. Thereby, an efficient computational framework is developed with an objective to model the uncertainties in response quantities of the base-isolated buildings. The specific objectives of the study are: (i) to determine the stochastic response of the base-isolated buildings considering uncertainties in the non-linear isolator and dynamic base excitation parameters; (ii) to study the efficiency of the gPC expansion technique for modeling the stochastic response of the base-isolated buildings; (iii) to investigate the effects on the stochastic response of the base-isolated buildings due to the equivalent linear elastic-viscous damping modeling and bi-linear hysteretic modeling approaches of the non-linear isolation system; (iv) to assess the influence of different uncertainty levels in the input parameters on the stochastic response quantities; and (v) to assess the influence of uncertainty in each input parameter on the uncertainty of the response quantities.

2. DETERMINISTIC MODEL OF BASE-ISOLATED BUILDINGS

Two base-isolated buildings are modeled as single degree of freedom (SDOF) system and five-storied multi degrees of freedom (MDOF) system. The details of their modeling are described in the following sections.

2.1 Modeling of base-isolated SDOF system

Schematic diagram of the base-isolated SDOF system is shown in Figure 1(a). The

superstructure is considered to be acting as a rigid mass, as studied earlier by Kulkarni and Jangid (2002 and 2003) and mostly so by Matsagar and Jangid (2006). The mass of the superstructure and base isolation system are lumped together. The governing equation of motion for the SDOF system under base excitation is given by

$$\left(m_b + \sum m_i\right)\ddot{x}_b + F_b = -\left(m_b + \sum m_i\right)\ddot{x}_g \quad (1)$$

where $\ddot{x}_b$ is the acceleration with respect to the ground at the isolator level; $m_b + \sum m_i$ is the total mass of the base isolation system and the total mass of the superstructure; F_b is the restoring force in the isolation system; and $\ddot{x}_g$ is the ground acceleration. The restoring force in the isolation system is inherently non-linear in nature. However, several international guidelines (ASCE-7 2016, IBC 2018) recommend use of the equivalent linear elastic-viscous damping modeling of the isolator. Nevertheless, bi-linear hysteretic modeling of the isolator force-deformation behavior is widely used to represent the non-linearity more accurately (Naeim and Kelly 1999). The following sections briefly describe the modeling approaches for the isolation system considered in this study.

2.1.1 *Equivalent linear elastic-viscous damping model*

International guidelines (ASCE-7 2016, IBC 2018) suggest a simplified equivalent linear elastic-viscous damping model for the isolator force-deformation behavior by defining an effective stiffness and effective damping. This modeling approach is referred as an equivalent linear model in this study for simplicity. The effective stiffness (k_{eff}) is calculated from the non-linear or actual force-deformation curve by taking slope of the line joining the positive peak (F^+, Δ^+) and negative peak (F^-, Δ^-) values as shown in Figure 1(b). The effective stiffness (k_{eff}) and effective viscous damping ratio (β_{eff}) of the isolator are defined in the codes as

$$k_{eff} = \frac{F^+ - F^-}{\Delta^+ - \Delta^-} \quad (2)$$

and $$\beta_{\text{eff}} = \frac{2}{\pi}\left[\frac{E_{\text{loop}}}{k_{\text{eff}}(|\Delta^{+}| + |\Delta^{-}|)^2}\right] \quad (3)$$

where E_{loop} represents the energy dissipation per cycle of loading. The restoring force developed in the isolator can be expressed as

$$F_{\text{b}} = c_{\text{eff}}\dot{x}_{\text{b}} + k_{\text{eff}}x_{\text{b}} \quad (4)$$

where the effective damping coefficient (c_{eff}) is expressed as

$$c_{\text{eff}} = 2\beta_{\text{eff}}\sqrt{k_{\text{eff}}M} \ . \quad (5)$$

Here, M is the total mass of the structure mounted on the base-isolators.

2.1.2 *Bi-linear hysteretic model*

Non-linear nature of the isolator force-deformation behavior is approximated through a bi-linear hysteretic force-deformation curve with the isolator parameters as shown in Figure 1(c). This modeling approach is referred as a bi-linear model in this study for simplicity. The bi-linear model can efficiently represent most of the isolation systems currently used in practice. The characteristics of the bi-linear hysteresis loop can be expressed in terms of three parameters; namely, (i) characteristic strength (Q), (ii) yield displacement (q), and (iii) post-yield stiffness (k_{b}). Post-yield stiffness is generally selected to obtain a specific value of time period of the isolation system (i.e., $T_{\text{b}} = 2\pi\sqrt{M/k_{\text{b}}}$). In the equivalent linear elastic model for a bi-linear hysteresis loop, the effective stiffness and damping ratio at a specific value of design isolation displacement (D), are expressed as

$$k_{\text{eff}} = k_{\text{b}} + \frac{Q}{D} \quad (6)$$

and $$\beta_{\text{eff}} = \frac{2Q(D-q)}{\pi k_{\text{eff}}D^2} \ . \quad (7)$$

It can be noted here that, an iterative process is required to arrive at desired isolation time period and design displacement (Naeim and Kelly 1999). However, at a given design

displacement, the characteristics of a bi-linear hysteresis loop can be defined by three independent quantities, i.e., Q, q, and k_b. Instead of using Q, q, and k_b from Eqs. (6) and (7), it is evident that an alternate set of variables, namely (i) effective stiffness (k_{eff}) or effective time period $\left(T_{eff} = 2\pi\sqrt{M/k_{eff}}\right)$, (ii) effective damping ratio (β_{eff}), and (iii) yield displacement (q) can be used.

2.2 Modeling of base-isolated MDOF system

A five-story base-isolated building is considered as an example MDOF system for the present study. The building is modeled as a shear building with one lateral degree of freedom at each floor level, and one degree of freedom corresponding to the base isolation system. A schematic diagram of the base-isolated five-story building is shown in Figure 1(d), where m_i and k_i represent the total mass and stiffness of i^{th} story. The rotational degrees of freedom are not taken into consideration. The modeling assumptions for the structural system are adopted from Matsagar and Jangid (2004) as listed below.

(i) The superstructure is considered to remain reasonably within the elastic limit during the ground excitation. The introduced isolation system attempts to reduce the earthquake response in such a way that the structure remains within the elastic range.

(ii) The floors are assumed rigid in its own plane owing mainly to the diaphragm action and the mass is lumped at each floor level.

(iii) The lateral stiffness is provided by the columns that are inextensible and weightless, whereas their mass is added in the adjoining floor masses.

(iv) A single horizontal component of earthquake ground motion is experienced by the base-isolated structure.

(v) The effects of soil-structure interaction (SSI) are not considered in the present study.

The governing equations of motion for the superstructure are obtained by equating the forces at each floor level, and expressed in matrix form as

$$[M_s]\{\ddot{x}_s\}+[C_s]\{\dot{x}_s\}+[K_s]\{x_s\}=-[M_s]\{r\}(\ddot{x}_g+\ddot{x}_b) \quad (8)$$

where $[M_s]$ is the mass matrix, $[C_s]$ is the damping matrix, $[K_s]$ is the stiffness matrix, $\{r\}$ is the vector of influence coefficients, and $\ddot{x}_b$ is acceleration at isolation level with respect to the ground. The displacement, velocity, and acceleration vectors relative with respect to the isolation level are given by $\{x_s\}=\{x_1,x_2,x_3,x_4,x_5\}^T$, $\{\dot{x}_s\}$, and $\{\ddot{x}_s\}$, respectively. The governing equation of motion for the base mass (m_b) is expressed as

$$m_b\ddot{x}_b+F_b-c_1\dot{x}_1-k_1x_1=-m_b\ddot{x}_g \quad (9)$$

where F_b is the restoring force developed in the isolator, c_1 and k_1 are the first-story damping coefficient and stiffness, respectively.

2.3 Important output parameters of seismic response

The output parameters investigated in this study are the displacement at the isolation level - bearing displacement and the acceleration at the top floor level - top floor acceleration. For the design of a base isolation system, computing the isolation displacement accurately is essential when used for the seismic protection of structures. Also, it is crucial for estimating the separation gap distance (moat width) between the base-isolated structure and the adjacent base-isolated / fixed-base structures to avoid consequences of pounding (Matsagar and Jangid 2003). Estimation of the peak isolation displacement with quantified uncertainty hence becomes more important in the design of the base-isolated structures. The effectiveness of the base isolation system in mitigating the seismic effects can be directly estimated from the top floor acceleration, in addition to the story drift obtained from the relative floor displacements. The seismic base shear induced in the columns of the building is proportional to the top floor acceleration. Floor acceleration is also a measure of human comfort in the base-isolated building during the unfortunate event of an earthquake, as well as protection of secondary systems and equipment housed within a base-isolated building. Hence, bearing displacement

and top floor acceleration are the two seismic response quantities of interest in the present study as global outputs. The 3D behavior of the structure is not considered in the MDOF system modeling and the masses are lumped at the floor level. The 3D effects are neglected in the deterministic modeling as base-isolated buildings are generally designed to have predominant translational mode of vibration; i.e., lengthening of time period in horizontal - translational direction.

3. STOCHASTIC MODELING USING gPC EXPANSION TECHNIQUE

Considering the base excitation as a sinusoidal input with amplitude A and frequency ω, Eqs. (1) and (4) can be combined and rewritten as

$$\left(m_b + \sum m_i\right)\ddot{x}_b + c_{eff}\,\dot{x}_b + k_{eff}\,x_b = -\left(m_b + \sum m_i\right)A\sin(\omega t)\,. \tag{10}$$

In the present study, the isolator parameters and the excitation parameters are considered uncertain. Therefore, Eq. (10) is rewritten with stochastic variables as

$$\ddot{x}_b(t,\xi) + 2\overline{\omega}(\xi_1)\beta_{eff}(\xi_2)\,\dot{x}_b(t,\xi) + \left\{\overline{\omega}(\xi_1)\right\}^2 x_b(t,\xi) = -A(\xi_3)\sin\left\{\omega(\xi_4)t\right\} \tag{11}$$

where $\dot{x}_b(t,\xi)$ and $x_b(t,\xi)$ are the unknown uncertain velocity and displacement at the isolation level relative to the ground, respectively; $\overline{\omega} = 2\pi / T_{eff} = \sqrt{k_{eff} / \left(m_b + \sum m_i\right)}$ is the natural frequency of the isolator; and $\xi = \{\xi_1, \xi_2, \xi_3, \xi_4\}$ is the random vector.

The bearing displacement, i.e., the displacement at the isolation level, is a function of time and the random vector, $\xi = \{\xi_1, \xi_2, \xi_3, \xi_4\}$. The elements of the random vector (ξ), ξ_1, ξ_2, ξ_3, and ξ_4 represent the uncertainties in time period (T_{eff}), damping ratio (β_{eff}), amplitude (A), and frequency (ω) of the base excitation function, respectively. The random variables are assumed to be independent and identically distributed (iid). For the bi-linear modeling approach, the isolator yield displacement (q) is also considered as an additional uncertain parameter. Therefore, the random vector (ξ) consists of five elements (ξ_1, ξ_2, ξ_3, ξ_4, and ξ_5) when the bi-linear isolator modeling approach is considered.

3.1 Solution of stochastic equation of motion

In the gPC expansion technique, the input as well as the output uncertain parameters are represented by a truncated polynomial series. The basic idea is to find out how uncertainties in the input parameters propagate to the output parameters. The j^{th} input uncertain parameter (P_j) is represented by the gPC expansion as (Ghanem and Spanos 1993)

$$P_j \approx \sum_{i=0}^{N_t} p_i \Phi_i(\xi_j) \tag{12}$$

where p_i represents the gPC expansion coefficient and $\Phi_i(\xi_j)$ is the orthogonal basis used to model the uncertainty. Here, N_t represents the highest order of the orthogonal basis used to approximate the uncertain input parameter. For normally distributed independent parameters, Hermite polynomials are best suited as the orthogonal basis (Xiu and Karniadakis 2002, Sepahvand et al. 2010). The gPC expansion coefficients of Eq. (12) can be obtained using the orthogonality property of the Hermite polynomials (H_i) and employing random Galerkin projection as

$$p_i = \frac{1}{\left\langle H_i^2 \right\rangle} \int_{-\infty}^{\infty} P_j H_i(\xi_j) \rho(\xi_j) d\xi_j \tag{13}$$

where $\left\langle H_i^2 \right\rangle$ denotes the inner product and norm of the polynomial, and $\rho(\xi_j)$ is the PDF of the j^{th} variable.

In the next step, the output response (Y_j) is also represented by a truncated gPC expansion as

$$Y_j \approx \sum_{i=0}^{P} y_i \Psi_i(\xi) \tag{14}$$

where y_i represents the gPC expansion coefficient and $\Psi_i(\xi)$ is the orthogonal basis, represented by all the uncertain input parameters used to model the uncertainty. Here, (P+1) represents total number of terms in the gPC expansion, which is related to the highest order of the orthogonal basis, N_t used to approximate the uncertain output parameter.

For multivariate cases, the orthogonal basis $[\Psi_i(\xi)]$ includes combination of different polynomial basis representing each uncertain parameter. For an example, the orthogonal basis (considering Hermite polynomials) corresponding to a second order expansion over two random dimensions are given as

$$\begin{aligned}
\Psi_0(\xi) &= H_0(\xi_1)H_0(\xi_2) = 1, \\
\Psi_1(\xi) &= H_1(\xi_1)H_0(\xi_2) = \xi_1, \\
\Psi_2(\xi) &= H_0(\xi_1)H_1(\xi_2) = \xi_2, \\
\Psi_3(\xi) &= H_2(\xi_1)H_0(\xi_2) = \xi_1^2 - 1, \\
\Psi_4(\xi) &= H_1(\xi_1)H_1(\xi_2) = \xi_1\xi_2, \\
\Psi_5(\xi) &= H_0(\xi_1)H_2(\xi_2) = \xi_2^2 - 1.
\end{aligned} \tag{15}$$

Now, the deterministic coefficients (y_i) of the gPC expansion of the output parameters are to be obtained. Two classes of methods are widely used to solve for the gPC expansion coefficients, such as (i) intrusive method and (ii) non-intrusive method.

A Galerkin projection scheme is used in the intrusive method taking advantage of the orthogonality property of the base function $[\Psi_i(\xi)]$. Unlike in the intrusive method, in the non-intrusive method the structural model is maintained non-intervened. No knowledge of governing equations is needed in this solution procedure. Hence, this method is quite useful for finite element (FE) models where the governing equations are not always explicitly known. Systems having non-linearity or systems with complex stochastic equations can also be analyzed with ease through this method. Based on the least squares minimization of the discrepancy between the uncertain parameter and its truncated gPC expansion, a well-known approach is collocation method. Saha et al. (2013) presented a step-by-step procedure to solve the stochastic equations of the base-isolated liquid storage tanks in time domain using the collocation-based non-intrusive method for linear isolator force-deformation behavior. Here, similar approach is adopted, however with a modified scheme for selection of the collocation points which is more efficient in case of a multivariate problem, required specifically for the

non-linear force-deformation behavior of the isolation system.

3.2 Selection of collocation points: sparse grid approximation

For multivariate problems, it is common to select judicially smaller number of collocation points from the full tensor product space. Since the number of points in the full tensor product grid increases exponentially with the dimension, these grids suffer from the curse of dimensionality. In the collocation method, the system is treated as a black box and the solution of the governing equations is determined at selected points, called the collocation points. Different strategies are available in the literature for the selection of the collocation points.

3.2.1 *Random points*

The requirement of the choice of the collocation point is that the system of linear equation is well-conditioned. One way of choosing such points is selecting them at random. Although it is convenient to choose the collocation points at random, it is not guaranteed that an accurate and consistent solution is obtained in each run. Numerical instabilities may arise due to clustering of the collocation points. In the present work, the collocation points are chosen in such a way that they are the solutions of the orthogonal basis (Hermite polynomials).

3.2.2 *Full tensor product*

The collocation points are chosen in the way described above for uni-variate problems. However, in multivariate problems, i.e., for problems with more than one variable uncertain, a common methodology adopted is to use collocation points of the full tensor product space. The computational cost of the full tensor product increases enormously with the increase in the number of random variables, which is referred to as the curse of dimensionality (Fish and Wu 2011).

3.2.3 *Sparse grid*

If the number of random variables is moderately large, a sparse grid approximation is a superior choice over a full tensor product (Smolyak 1963). This method leads to a great amount of

computational saving, as the number of collocation points is less as compared to the full tensor product. Let, Θ^{i_1} be the vector of collocation points in one-dimensional space. For multivariate problems of order *n*, the full tensor product approach considers all points in the full tensor product space obtained from

$$U = \Theta^{i_1} \otimes \Theta^{i_2} \ldots \otimes \Theta^{i_n} . \tag{16}$$

Considering all the vectors have *d* elements, the number of points in the resulting space is d^n. It is clearly seen that as *n* increases, number of points in the tensor product space increases exponentially. In the sparse grid approximation, we set $|i| = i_1 + i_2 + \ldots + i_n$, then the number of points in the sparse grid ($H_{\kappa, N}$) is defined as (Ganapathysubramanian and Zabaras 2007)

$$H_{\kappa,N} = \underset{\kappa - N+1 \le |i| \le \kappa}{U} (\Theta^{i_1} \times \Theta^{i_2} \ldots \times \Theta^{i_n}) \tag{17}$$

where *N* is the number of stochastic dimension and (κ-*N*) is the order of interpolation.

Hence, we need to evaluate the function value only at these points in the sparse grid. Figure 2 shows an example of the full tensor product space and the sparse grid for a two variable system with 4th order interpolation. Same level of accuracy can be achieved with considerably smaller number of analyses of the structural model leading to substantially reduced computational effort. This difference is especially crucial for higher dimension problems.

3.3 Non-intrusive gPC method-based on sparse grid collocation

Based on the sparse grid collocation, the non-intrusive gPC method is employed here for quantifying effects of uncertainties in the dynamic response of the buildings equipped with non-linear base-isolators. Figure 3 depicts the step-by-step procedure followed for solving the current problem numerically.

3.3.1 *Uncertain parameter identification*

From the set of input parameters, those parameters having uncertain characteristics are identified. The behavior of any parameter is described by a probability measure such as the

PDF of the particular parameter under consideration. The PDF of the input uncertain parameter can be identified from experiments, observations, expertise, or experience. A standard distribution may also be assumed in cases where much experimental data is not available.

3.3.2 *Representation of input uncertain parameter*

The input uncertain parameters with a given PDF identified in the previous step are represented by a polynomial chaos (PC) expansion in terms of random vector, ξ. Since the input parameters are assumed normally distributed, they are best represented by the Hermite polynomials as

$$P_{\mathrm{j}}(\xi_{\mathrm{j}}) = \sum_{\mathrm{i}=0}^{\mathrm{N}} p_{\mathrm{j_i}} H_{\mathrm{i}}(\xi_{\mathrm{j}}) \tag{18}$$

where P_{j} represents each of the input uncertain parameters considered and $H_{\mathrm{i}}(\xi_{\mathrm{j}})$ represents the i^{th} Hermite polynomial.

3.3.3 *Determination of PC expansion coefficients of input parameters*

The PC expansion coefficients in Eq. (18) are determined easily by the Galerkin projection making use of the orthogonality of the Hermite polynomial.

$$p_{\mathrm{j_i}} = \frac{1}{\left\langle \Psi_{\mathrm{i}}^2 \right\rangle} \int_{\Omega} \left\langle P_{\mathrm{j}}, \Psi_{\mathrm{k}}(\xi) \right\rangle d\mu(\xi), \text{for } k = 1,\ 2,\ \cdots,\ N\,. \tag{19}$$

All other PC coefficients except p_{j0} and p_{j1} are found to be zero as Hermite polynomial is the optimum polynomial for Gaussian random variables. It may be noted that p_{j0} represents the mean of the distribution and p_{j1} represents the standard deviation of the input parameter, thus Eq. (19) leads to

$$P_{\mathrm{j}}(\xi_{\mathrm{j}}) = p_{\mathrm{j_0}} + p_{\mathrm{j_1}} \xi_{\mathrm{j}}\,. \tag{20}$$

3.3.4 *PC expansion for output parameters*

The output quantity of interest is also represented by a PC expansion as

$$Y(\xi) = \sum_{\mathrm{i}=0}^{\mathrm{P}} y_{\mathrm{i}} \Psi_{\mathrm{i}}(\xi)\,. \tag{21}$$

The PC coefficients have to be found out at each instant of time. Since a Hermite polynomial is used to approximate the input parameters, the same may be used for the output parameters as well. Therefore, Eq. (21) may be rewritten as

$$Y(t,\xi) = \sum_{i=0}^{P} y_i(t) H_i(\xi) . \tag{22}$$

For the given problem, the output response is represented by a 3rd order PC expansion. Here, $H_i(\xi)$ is the Hermite polynomial and is a function of the random variable vector, ξ. The random variable vector may contain more than one element depending upon the dimensionality of the random vector. In case of the multivariate problems, the orthogonal basis will be tensor product of the Hermite polynomials.

3.3.5 *Determination of PC expansion coefficients for input parameters*

The PC coefficients in Eq. (22) are determined by non-intrusive methods due to its simplicity and requiring lower computational time. The sparse grid is generated as per Eq. (17) corresponding to the dimension of the random space. Corresponding to each of the points in the sparse grid, input parameters are obtained from Eq. (18). The response of the deterministic model at these input parameter values are obtained by Newmark-β method at each time instant. A linear regression approach is adopted for finding out the PC coefficients. At each collocation point, Eq. (22) may be written, whereupon a set of equations equal to the number of collocation points in the sparse grid are obtained. Now,

$$\Psi\alpha = Y \tag{23}$$

where Ψ is a matrix of orthogonal basis values at the collocation points, α is a vector of unknown PC coefficients, and Y is a vector of responses at the collocation points. The number of collocation points should be at least equal to the number of unknown PC coefficients. If the number of equations is more than the number of unknowns, regression analysis based on the least squares approach is adopted to solve for α in Eq. (23). Now, knowing the PC coefficients of the output uncertain quantity, the stochastic response of the system is obtained. Convergence

criteria are checked, and additional PC terms are added if the convergence criteria are not met, and the abovementioned procedure is continued. The PDF of the output uncertain parameter and other statistical measures such as mean and standard deviation of the output uncertain quantity are then obtained.

4. NUMERICAL STUDY

Two idealized base-isolated SDOF and MDOF systems are considered for the present study to investigate the influence of the uncertainties in the isolator and excitation parameters on the dynamic response of the base-isolated buildings. The effective time period (T_{eff}), effective damping ratio (β_{eff}), and yield displacement (q) of the isolator are considered as the uncertain isolator parameters. On the other hand, the amplitude (A) and frequency (ω) of the sinusoidal excitation function are considered uncertain as well. In the present study, the terms 'isolation time period' and 'isolation damping' refer to the effective time period and effective damping of the isolation system, respectively. All the input parameters are assumed to follow normal distribution. The mean and standard deviation (SD) of the input parameters are shown in Table 1. The mean amplitude and mean frequency of the excitation (ground excitation - 1) function are assumed corresponding to the peak ground acceleration (PGA) and predominant frequency content of a recorded earthquake ground motion (N90S component of 1994 Northridge earthquake recorded at the Sylmar station). The design displacement (D) required for the bi-linear modeling of the isolator is assumed constant. It is computed as the peak spectral displacement of a SDOF system, having the dynamic properties T_{eff} and β_{eff}, when subjected to the sample recorded earthquake ground motion. The deterministic model is analyzed, and the solution is obtained using Newmark-β method for each set of collocation points. Total time of the excitation considered is 20 sec, and the time increment considered is 0.02/120 sec for linear and non-linear with q = 2.5 cm and 0.02/1000 for the case of $q = 10^{-4}$. The effects of the modeling approaches and the shape of the hysteresis loop of the isolator, on the propagation of

uncertainty from the input parameters to the response quantities, are investigated for both the SDOF and MDOF systems. Three different cases are compared for all the following numerical studies: (i) equivalent linear modeling of the isolator, defined by effective isolation time period (T_{eff}) and effective isolation damping ratio (β_{eff}); (ii) bi-linear modeling of the isolator with yield displacement, q = 2.5 cm, which represents an elastomeric system; and (iii) bi-linear modeling of the isolator with yield displacement, q = 10^{-4} cm, which represents a friction/ sliding system (onset of sliding mode from stick mode).

4.1 Response of base-isolated SDOF system

Stochastic response of the base-isolated SDOF system is determined using the gPC expansion technique based on the sparse grid collocation scheme. The amplitude of the excitation function is considered uncertain. The mean and standard deviation of the input parameters are considered as presented in Table 1. The bearing displacement (x_b) is the primary output parameter of interest for the base-isolated SDOF system. The output uncertain parameter is represented by a 3rd order gPC expansion. Figure 4 shows time histories for the coefficients of the gPC expansion for equivalent linear and bi-linear modeling approaches. It is observed that in all the cases the coefficient y_0, which denotes the mean value of the response, dominates over the other coefficients in magnitude. The coefficient y_1 is observed around 16% of y_0 only. The higher order coefficients are having substantially smaller values as compared to y_0 and y_1. Smaller values of y_2 and y_3 imply that the 3rd order gPC expansion is sufficient to estimate the stochastic bearing displacement of a base-isolated SDOF system. As reported by Field and Grigoriu (2004), the PC expansion method can diverge in certain strongly non-linear problems. In order to investigate such remarks, PDF of the peak bearing displacement for the equivalent linear and bi-linear models for different polynomials of order 3 (PC3) and 4 (PC4) are plotted in Figure 5. The PC expansion coefficients are obtained from regression approach. The PC3 and PC4 are observed to be in good agreement with each other showing convergence of the PC

expansion for both linear and bi-linear modeling approaches in predicting the peak bearing displacement.

4.1.1 *Probability measures of output uncertain parameter*

The gPC expansion coefficients and the probability distribution of the peak bearing displacement are obtained when the isolator is modeled using the equivalent linear and bi-linear modeling approaches considering all the input uncertain parameters as presented in Table 1. The response quantities are also compared with the same obtained using the MC simulation considering 10,000 sample points. The probability distribution of both the equivalent linear and bi-linear (with q = 2.5 cm and 10^{-4} cm) systems are compared in Figure 6. The deterministic peak bearing displacement, obtained using the mean values of the input parameters, is also shown for comparison. The mean value of the response obtained from the gPC and MC are also plotted. The maximum density of the peak response is observed near the deterministic values. However, the dispersion of the uncertain output is quite significant. The mean value of the response obtained is found to be higher than the deterministic values in both the equivalent linear and bi-linear isolator models. Moreover, the distributions of the peak bearing displacement, obtained using the gPC expansion, are in close agreement with that obtained using the MC simulation.

The probability distributions shown in Figure 6 clearly indicate that the gPC expansion technique is equally accurate in predicting the stochastic response of a base-isolated SDOF system for both the equivalent linear and bi-linear modeling approaches of the isolator. However, the accuracy of the MC simulation largely depends on the number of realizations and to achieve a reasonable convergence the deterministic model is evaluated for large set of input parameters.

Figure 7(a) shows the PDF of peak bearing displacement with increasing number of simulations for the equivalent linear modeling case. It can be noted that the shape of the PDF

converges as the number of simulations are increased. Figure 7(b) shows the variation in mean and standard deviation for the linear model of the SDOF system with number of MC simulations. It can be noted that the mean is found to converge at lower number of samples. However, the standard deviation is found to be requiring higher number of simulations to converge. Based on the results presented in these figures, 4,000 samples could be considered as sufficient in the current problem and is used for comparison of the computational cost with the gPC expansion based technique. Table 2 compares the computational time required for both the analyses using a computer with Intel® Core™ i3, 1.7 GHz processor, and 4 GB RAM. The gPC expansion technique consumes less than 15% of the computational time required for 4,000 MC simulations. Especially, when non-linearity in the considered isolation system is high, the computational effort for the MC simulations increases significantly. Therefore, it is concluded that, in order to achieve a considerable level of accuracy, in stochastic response analysis of the base-isolated structures, the gPC expansion technique can be suitably used with substantially less computational effort as compared to the MC simulation.

4.1.2 *Comparison of responses for equivalent linear and bi-linear models*

The mean and standard deviation of the peak bearing displacement, obtained using different modeling approaches of the isolator, are presented in Table 3. The mean value is found to be higher than the deterministic value in all the three cases. The mean value is about 4% higher than the deterministic value in case of the linear isolator. The mean value is about 15-17% higher than the deterministic value for the bi-linear models. These observations clearly indicate that the deterministic approach may not be sufficient to represent the response of the base-isolated building accurately in the presence of uncertainties in the isolator parameters. The response quantity may be underestimated leading to under-design, as most of the engineering practices utilize deterministic inputs for the design. Earlier, it was reported that the linear isolator model over-predicts the bearing displacement as compared to the bi-linear model

(Matsagar and Jangid 2004). Interestingly, the mean value of the bearing displacement obtained for the linear isolator model is found to be less than that of the bi-linear model. The uncertainties in the bi-linear isolator model parameters are responsible for this and indicate a need for the bi-linear modeling of the isolators. It is further observed that for the bi-linear model, standard deviation is higher than the equivalent linear model. This is possibly owing to the fact that in case of the bi-linear model, the uncertainty in the response is contributed by uncertainties in the five input parameters; whereas, for the equivalent linear model there are only four input parameters uncertain. As the dynamic response obtained using the equivalent linear model has lower standard deviation, it cannot accurately model the dispersion of the responses when the uncertainties in the input parameters are considered. This may have adverse consequences on probabilistic design of the base-isolated buildings, which essentially requires the mean and standard deviation of the response. This observation further strengthens the importance of a bi-linear modeling approach of the isolator over the equivalent linear modeling approach.

4.1.3 *Effect of different uncertainty levels*

The response of the base-isolated SDOF system is obtained to study the influence of uncertainty levels in the input parameters. For this study, only the amplitude of the excitation function is considered uncertain. The uncertain input parameter is assumed to have normal distribution with same mean value as given in Table 1; however, with different standard deviation values. Here, the standard deviation (SD) is expressed as percentage of the mean value. The probability distributions of the bearing displacement for different levels of the uncertainties are presented in Figure 8.

It is evidently observed that, as the level of uncertainty increases, the dispersion of the peak bearing displacement also increases, i.e., higher SD for higher level of uncertainty. It is also observed that the symmetry in the distribution, present at lower uncertainty level, is lost when

the level of uncertainty increases, especially for the bi-linear modeling approach of the isolator. Therefore, selection of appropriate level of uncertainties is important for accurate estimation of the stochastic response of the base-isolated structures.

4.1.4 *Effect of individual input parameter uncertainty*

The uncertainty of the output parameter is contributed by the uncertainties in the various input parameters. To ascertain the effects of individual input parameters on the response statistics, uncertainty in one input parameter is considered at a time. Mean and standard deviation of the input parameters are considered as presented in Table 1. All other input parameters are assumed to have deterministic values equal to their mean values. The probability distribution of the output parameter, bearing displacement, is obtained using 3rd order gPC expansion. The distributions obtained, considering individual uncertain parameter, are compared in Figure 9. The distribution, with damping ratio (β_{eff}) as uncertain parameter, has least dispersion from the peak in all three cases, i.e., equivalent linear model, bi-linear model with q = 2.5 cm, and bi-linear model with q = 10^{-4} cm. It can be observed that all the considered parameters have noticeable influence on the response distribution. For the bi-linear isolator model, the yield displacement (q) has also shown noticeable influence, which cannot be captured when the equivalent linear model of the non-linear isolator is adopted in the dynamic analysis. The deviation from the mean is considerably more for isolation time period (T_{eff}), frequency (ω) and amplitude (A) of the excitation function, indicating that these parameters have major influence on the response. Thus, varying effects of the individual input parameter uncertainty are observed, demonstrating that each one of them require separate attention depending upon how sensitive the dynamic response to the uncertain input parameter is. Therefore, sensitivity analysis is carried out to quantify the effect of the individual parameter uncertainty.

4.1.5 *Sensitivity analysis for SDOF system*

One of the major advantages of the gPC expansion technique over the MC simulation is that,

in the former case, a series expansion is formulated in order to represent the stochastic response of the output random variable at the end of the solution process. Since the response is known explicitly, it is easier to calculate higher order moments, and use the resulted gPC expansion for sensitivity analysis. Sensitivity analysis quantifies how the uncertainty of the output random variable can be apportioned to different sources of uncertainty in the input parameters. It provides a better understanding of the relationships between the input parameters and output response in any stochastic model. The sensitivity analysis includes determining derivative of the output uncertain parameters with respect to the input uncertain parameters. The sensitivity of the uncertain peak response (Y_i) towards j^{th} input parameters (S_j) is given by

$$S_j = \frac{dY_i}{dP_j} = \frac{dY_i}{d\xi}\frac{d\xi}{dP_j}. \tag{24}$$

If the assumption of independent and identically distributed (iid) random variables is made, Eq. (24) leads to

$$S_j = \frac{dY_i}{dP_j} = \frac{dY_i}{d\xi_j}\frac{d\xi_j}{dP_j}. \tag{25}$$

Contribution of each input uncertain parameter (S) towards uncertainty in the peak bearing displacement of the base-isolated SDOF system is quantified in percentage, and shown in Figure 10. As observed in the previous section, the isolation time period (T_{eff}) as well as the amplitude (A) and frequency (ω) of the excitation have major contribution towards the uncertainty in the peak bearing displacement of the base-isolated SDOF system in both the equivalent linear and bi-linear isolator modeling approaches. The isolation time period has the maximum contribution towards uncertainty in the bearing displacement.

It is observed that the yield displacement (q) has considerable influence on the bearing displacement when the bi-linear modeling approach is considered. The effect of uncertainty in the yield displacement is marginally more for elastomeric isolation system (q = 2.5 cm) than the friction isolation system ($q = 10^{-4}$ cm). As the yield displacement increases, the contribution

towards the uncertainty in the bearing displacement is also increased. A significant amount of uncertainty in the bearing displacement can be apportioned to the yield displacement (q) and isolation time period (T_{eff}), two major parameters that control the shape of the bi-linear hysteresis loop.

4.1.6 Global sensitivity analysis

A global sensitivity analysis is carried out in order to find out how uncertainties in the model output can be apportioned to uncertainties in the input parameters that are considered over the entire range of the input parameters. In the global sensitivity analysis, uncertainties due to the combination of the parameters are considered. Unlike local sensitivity analysis, the effect throughout the entire parameter space is considered in the global sensitivity analysis. Global sensitivity analysis approaches can be divided into two groups as (a) regression-based methods and (b) variance-based methods.

Sobol' indices are a variance-based method and they provide accurate information of sensitivity in most of the models and have received lot of attention in the recent times. Sudret (2008) presented a method to calculate the Sobol' indices from polynomial chaos expansion. The Sobol' indices based on polynomial chaos (PC) are determined from the PC expansion with negligible additional computational cost. The variance from the PC expansion, D_{PC}, can be calculated as

$$D_{\text{PC}} = \sum_{\text{j=1}}^{\text{P}} f_{\text{j}}^2 E[\psi_{\text{j}}^2]. \tag{26}$$

The response expansion coefficients are gathered according to the dependency of each basis polynomial, square summed, and normalized to obtain the PC based Sobol' indices. The total sensitivity indices are computed by summing up the corresponding Sobol' indices as reported in Sudret (2008). The total PC-based Sobol' indices, S_{j}^{T}, of j^{th} input parameter with random vector ξ_{j} can be determined as

$$S_j^T = \sum y_\lambda^2 E[\psi_\lambda^2(\xi)] / D_{PC} \quad (27)$$

where λ denotes all indices, such that $\psi_\lambda(\xi)$ is dependent on ξ_j.

Sobol' indices are computed toward the peak bearing displacements for the base-isolated SDOF system and the total indices are shown in Table 4. It is observed that the peak bearing displacement is mainly influenced by the isolation time period, as well as amplitude and frequency of the excitation. Further, it is interesting to note that, in the presence of similar level of uncertainty in the isolation time period, the other isolation parameters (damping and yield displacement) do not show noticeable influence on the bearing displacement.

4.2 Response of MDOF system

A five-story base-isolated building [Figure 1(d)] is considered as MDOF system for the present study. The stochastic response of the MDOF system is obtained by approximating the response quantities using 3rd order gPC expansion. The response quantities of interest are the top floor acceleration (a) and the bearing displacement (x_b). The top floor acceleration is an indicator of the force exerted on the superstructure due to the ground excitation. Also, the bearing displacement is critical for the design of the base isolation system. The mass of each floor is kept constant and taken same as the base mass (m_b). The damping ratio of the superstructure is assumed to be constant (0.02) in all modes of vibration. The damping matrix of the base-isolated building is not explicitly known, and it is calculated from the assumed damping ratio of the superstructure and isolator. The inter-story stiffness k_1, k_2, k_3, k_4, and k_5 are taken in proportions of 3, 2.5, 2, 1.5, and 1, respectively. The absolute inter-story stiffness is calculated in such a way that the fixed-base superstructure has a specified fundamental period (T_s = 0.5 sec).

4.2.1 ***Statistical measure of output uncertain parameters***

The probability distributions of the peak top floor acceleration and peak bearing displacement,

obtained using 3rd order gPC expansions and 10,000 MC simulations, are shown in Figure 11. The equivalent linear and bi-linear modeling approaches for the isolator are considered. The input parameters for the isolation system and the base excitation are considered same as that presented in Table 1 earlier. It is observed that the distributions of the dynamic response obtained using 3rd order gPC expansion closely resembles to that obtained using the MC simulations. The density of the peak bearing displacement and peak top floor accelerations are observed maximum near the deterministic values. The peak response quantities, obtained using the bi-linear model of the isolator, are observed to have higher dispersion from the deterministic values as compared to that obtained using the equivalent linear model of the isolator. The mean and standard deviation of the peak response quantities for the base-isolated MDOF system, obtained using the gPC expansion technique and MC simulations are presented in Table 5. The deterministic peak response quantities are also presented for comparison. It is observed that the deterministic response quantities are less than the mean response quantities, obtained from the stochastic analyses, in all the cases. Therefore, deterministic approach is not sufficient to represent accurately the peak response of a multistory base-isolated building (MDOF system). The response quantities, obtained using deterministic analyses, may underestimate the peak responses leading to under-design.

4.2.2 *Comparison of responses for equivalent linear and bi-linear models*

The mean and standard deviation of the quantities of interest (i.e., bearing displacement and top floor acceleration) are tabulated in Table 5. Although, the mean values are found to be higher than the deterministic value for both the modeling approaches of the isolator; the mean values of the bearing displacement obtained using the equivalent linear isolator model are found to be less than those obtained using the bi-linear model. It is further observed that the peak response quantities, when equivalent linear model is considered, have lower standard deviation. Therefore, the uncertainty in the peak response of the base-isolated building may be

underestimated when the equivalent linear modeling is adopted for isolator modeling. Therefore, the bi-linear modeling approach of the isolator is recommended, over the equivalent linear isolator model, for more accurate estimation of the peak response statistics.

4.2.3 *Effect of different uncertainty levels*

Effects of variation in uncertainty levels of the input parameters on the peak bearing displacement and peak top floor acceleration are investigated. Analyses are carried out keeping the amplitude of the sinusoidal excitation as uncertain with the mean given in Table 1. However, the standard deviation is increased from 10% to 40% of its mean. The probability distributions of the peak bearing displacement and the peak top floor acceleration are presented in Figure 12. It is observed that as the level of uncertainty increases, the dispersion of the peak response quantities also increases. As the uncertainty in the input parameters increases, the symmetry of the distribution about the mean response, present at lower uncertainty level, is lost. Notably, the distribution of the peak top floor acceleration appears to maintain symmetry even at higher levels of the uncertainties. Therefore, it is concluded that the bearing displacement in the MDOF system is more sensitive to the uncertainty level of the input parameters as compared to the top floor acceleration. This is crucial from viewpoint of design of the base isolation systems for protection of displacement- and acceleration-sensitive secondary equipment contained in the base-isolated structures.

4.2.4 *Effect of individual input parameter uncertainties*

The uncertainties in the peak bearing displacement and peak top floor acceleration are contributed from the uncertainties in various input parameters of the isolator and excitation function. To ascertain the effect of individual input parameters on the response statistics, uncertainty in only one input parameter is considered at a time (as given in Table 1). All other input parameters are kept deterministic at their mean values. The probability distributions of the output parameters (peak bearing displacement and peak top floor acceleration) are obtained

by 3rd order gPC expansion and compared in Figure 13.

For peak bearing displacement, the behavior is similar to that of the SDOF system response, as observed and discussed earlier. All the considered uncertain parameters have noticeable influence on the peak bearing displacement. Distribution of the peak top floor acceleration is also influenced by the considered uncertain parameters. However, the spread of the distribution (representing standard deviation) of the peak response is observed to be small as compared to that for the bearing displacement. Moreover, it is also observed that the uncertainties in the excitation parameters have larger influence on the distribution of the peak top floor acceleration as compared to the uncertainties in the isolation system parameters.

4.2.5 *Sensitivity analysis for MDOF system*

Sensitivity analyses are carried out by taking derivatives of the gPC expansions corresponding to the output parameters with respect to the individual uncertain input parameters. The sensitivity of each of the input parameters is represented in percentage and is shown in Figure 14. It is observed that the isolation time period (T_{eff}) as well as amplitude (A) and frequency (ω) of the sinusoidal excitation are the major contributors towards the uncertainty in the peak bearing displacement of the base-isolated MDOF system. Whereas, the importance of bi-linear modeling is further ascertained by the significant contribution of the yield displacement towards the uncertainty in the peak bearing displacement. As expected from the observations made in the previous section, uncertainty in the peak top floor acceleration is found to be influenced more by the uncertainties in the excitation function as compared to the uncertainties in the isolation parameters.

4.2.6 *Global sensitivity analysis for MDOF system*

The total Sobol' indices for the peak bearing displacement and top floor acceleration are computed using Eq. 27 and presented in Tables 6 and 7, respectively. As observed in case of the SDOF system, the uncertainties in the peak bearing displacement are primarily contributed

by the isolator time period as well as the amplitude and frequency of the excitation. However, in the presence of similar uncertainty level in the time period, the effect of uncertainties in the other parameters of the isolator (e.g., damping and yield displacement) is comparatively less. Moreover, the uncertainties in the peak top floor acceleration is primarily contributed by the uncertainties in the excitation function. It suggests that reducing uncertainty in the top floor acceleration in building is difficult owing to the uncontrollable uncertainty in the forcing function parameters of the earthquake ground motion.

4.2.7 *Effect of superstructure damping*

For the current study, the damping for the base-isolated steel superstructure is assumed 2%, which is close to the material damping, as the superstructure is not expected to have any non-linear deformation. However, in this section the effect of the superstructure damping is studied by considering 2% and 5% damping for the superstructure. The PDF of both 2% and 5% damping cases are plotted in Figure 15. It can be seen that distribution of both the peak bearing displacement and the peak top floor acceleration are meagerly influenced by the superstructure damping. The mean value and standard deviation are found to be marginally less compared to 2% owing to the increased damping of the system.

4.2.8 *Effect of amplitude and frequency of ground excitations*

To investigate the effect of amplitude and frequency of the ground excitation on the stochastic response of the base-isolated structure, three sets of amplitude and frequency corresponding to three recorded earthquake ground motions are considered apart from the one presented in Table 1. The mean and standard deviation of the amplitude and frequency of the ground excitation and the details of the considered earthquakes are tabulated in Table 8. Other uncertain input parameters relating to the structures are considered same as given in Table 1. The deterministic values of the mean and standard deviation of the peak bearing displacement and top floor acceleration of the base-isolated MDOF system is tabulated in Table 9. The PDF

of the bearing displacement and the top floor acceleration are shown in Figures 16, 17, and 18. The deterministic value and mean value are also plotted in the figures for clarity. It can be observed that in majority of the cases the deterministic value is less than the predicted mean value of the distribution as observed for ground excitation - 1.

The Sobol' indices are tabulated in Table 10 for all the three base excitations. It can be observed as before that the bearing displacement is mostly influenced by the amplitude and frequency of the base excitation and the time period of the base isolation system. The uncertainties in the top floor acceleration are majorly influenced by the frequency content of the base excitation function. The top floor acceleration is less influenced by the uncertainties in the system parameters. These observations are also in line with that made using ground excitation - 1.

5. CONCLUSIONS

An efficient framework is developed to model stochastic response of base-isolated building using generalized polynomial chaos (gPC) expansion technique. The uncertain input parameters and the response quantities are represented by the truncated gPC expansion. Non-intrusive sparse grid collocation scheme is used to obtain the gPC expansion coefficients corresponding to the peak response quantities. The probability distributions of the peak response quantities obtained using the gPC expansion technique and MC simulation are compared. The influences of the isolator modeling approaches on the estimation of the response statistics are also investigated. Variation of the peak response distributions with different levels of uncertainties in the input parameters is studied. Sensitivity analyses are also carried out to quantify the contribution of each uncertain input parameter towards the uncertainty in the peak response quantities. Based on this numerical investigation, the following conclusions are drawn.

i. The presented numerical framework based on the gPC expansion technique is computationally efficient yet accurate alternative to the MC simulation for uncertainty

quantification in the dynamic analyses of the base-isolated buildings.

ii. The mean values of the peak bearing displacement and peak top floor acceleration are significantly higher as compared to the deterministic peak responses when uncertainties in the input parameters are considered. This indicates that the design based on the deterministic analysis may lead to unsafe premise.

iii. Equivalent linear elastic-viscous damping model of the isolator underestimates the standard deviations of the peak response quantities. This may have adverse consequences on the probabilistic design of the base-isolated buildings.

iv. The shape of the hysteresis loop has a considerable contribution towards the uncertainty in the bearing displacement calculation, which is not captured under the equivalent linear elastic-viscous damping isolator model.

v. The uncertainties in the excitation function parameters primarily influence the uncertainty in the peak top floor acceleration. However, uncertainty in the bearing displacement is mainly influenced by the uncertainties present in the isolator parameters as well as in the excitation parameters.

6. ACKNOWLEDGEMENTS

The financial supports received from the Deutscher Akademischer Austausch Dienst (DAAD) and the Alexander von Humboldt (AvH) Foundation for carrying out the reported research are gratefully acknowledged.

7. REFERENCES

Ahmadi, G. (1983), "Stochastic earthquake response of structures on sliding foundation", *International Journal of Engineering Science*, 21(2), 93-102.

Alhan, C.; and Gavin, H.P. (2005), "Reliability of base-isolation for the protection of critical equipment from earthquake hazards", *Engineering Structures*, 27(9), 1435-1449.

Amadio, C.; Rinaldin, G.; and Fragiacomo, G. (2016), "Investigation on the accuracy of the

N2 method and the equivalent linearization procedure for different hysteretic models", *Soil Dynamics and Earthquake Engineering*, 83, 69-80.

ASCE-7 (2016), "Minimum design loads for buildings and other structures", American Society of Civil Engineers (ASCE), Virginia (VA), USA.

Buckle, I.G.; and Mayes, R.L. (1990), "Seismic isolation history, application and performance - a world review", *Earthquake Spectra*, 6(2), 161-202.

Field, R.V.; Grigoriu, M. (2004) "On the accuracy of the polynomial chaos approximation", *Probabilistic Engineering Mechanics*, 19, 65-80.

Fish, J.; and Wu, W. (2011), "A non-intrusive stochastic multi-scale solver", *International Journal for Numerical Methods in Engineering*, 88, 862-879.

Ganapathysubramanian, B.; and Zabaras, N. (2007), "Sparse grid collocation schemes for stochastic natural convection problems", *Journal of Computational Physics*, 225(1), 652-685.

Ghanem, R.; and Spanos, P. (1993), "A stochastic Galerkin expansion for non-linear random vibration analysis", *Probabilistic Engineering Mechanics*, 8(3-4), 255-264

Greco, R.; and Marano, G.C. (2016), "Robust optimization of base isolation devices under uncertain parameters", *Journal of Vibration and Control*, 22, 853-868.

IBC (2018), "International building code", International Code Council, Inc., Illinois (IL), USA.

Jacob, C.M.; Sepahvand, K.; Matsagar, V.A.; and Marburg, S. (2013), "Stochastic seismic response of base-isolated buildings", *International Journal of Applied Mechanics*, 5(1), 1-21.

Jangid, R.S. (2000), "Stochastic seismic response of structures isolated by rolling rods", *Engineering Structures*, 22(8), 937-946.

Jangid, R.S.; and Datta, T.K. (1995a), "Seismic behavior of base-isolated building: a state-of-the-art-review", *Structures and Buildings*, 110(2), 186-203.

Jangid, R.S.; and Datta, T.K. (1995b), "Performance of base-isolation systems for asymmetric building subject to random excitation", *Engineering Structures*, 17(6), 443-454.

Kelly, J.M. (1986), "Aseismic base-isolation: review and bibliography", *Soil Dynamics and Earthquake Engineering*, 5(4), 202-216.

Kulkarni, J.A.; and Jangid, R.S. (2002), "Rigid body response of base-isolated structures", *Journal of Structural Control*, 9(3), 171-188.

Kulkarni, J.A.; and Jangid, R.S. (2003), "Effects of superstructure flexibility on the response of base-isolated structures", *Shock and Vibration*, 10, 1-13.

Li, J.; and Chen, J.B. (2004), "Probability density evolution method for dynamic response analysis of structures with uncertain parameters", *Computational Mechanics*, 34(5), 400-409.

Markou, A.A.; Stefanou, G.; and Manolis, G.D. (2018), "Stochastic response of structures with hybrid base isolation systems", *Engineering Structures*, 172, 629-643.

Markou, A.A.; Stefanou, G.; and Manolis, G.D. (2019), "Stochastic energy measures for hybrid base isolation systems", *Soil Dynamics and Earthquake Engineering*, 119, 454-470.

Matsagar, V.A.; and Jangid, R.S. (2003), "Seismic response of base-isolated structures during impact with adjacent structures", *Engineering Structures*, 25(10), 1311-1323.

Matsagar, V.A.; and Jangid, R.S. (2004), "Influence of isolator characteristics on the response of base-isolated structures", *Engineering Structures*, 26(12), 1735-1749.

Matsagar, V.A.; and Jangid, R.S. (2006), "Dynamic characterization of base-isolated structures using analytical shear-beam model", *International Journal of Acoustics and Vibration*, 11(3), 132-136.

Naeim, F.; and Kelly, J.M. (1999), "Design of seismic isolated structures: from theory to practice", John Wiley & Sons Inc., New York (NY), USA.

Saha, S.K.; Sepahvand, K.; Matsagar, V.A.; Jain, A.K.; and Marburg, S. (2013), "Stochastic

analysis of base-isolated liquid storage tanks with uncertain isolator parameter under random excitation", *Engineering Structures*, 57, 465-474.

Schuëller, G.I.; and Pradlwarter, H.J. (2009), "Uncertainty analysis of complex structural systems", *International Journal for Numerical Methods in Engineering*, 80(6-7), 881-913.

Sepahvand, K.; Marburg, S.; and Hardtke, H.-J. (2010), "Uncertainty quantification in stochastic systems using polynomial chaos expansion", *International Journal of Applied Mechanics*, 2(2), 305-353.

Smolyak, S. (1963), "Quadrature and interpolation formulas for tensor products of certain classes of functions", Doklady Akademii Nauk SSSR, 4, 240-243.

Sudret, B. (2008), "Global sensitivity analysis using polynomial chaos expansions", *Reliability Engineering and System Safety*, 93, 964-979.

Warn, G.P.; and Ryan, K.L. (2012), "A review of seismic isolation for buildings: historical development and research needs", *Buildings*, 2(3), 300-325.

Wiener, N. (1938), "The homogeneous chaos", *American Journal of Mathematics*, 60(4), 897-936.

Xiu, D.; and Karniadakis, G. (2002), "The Wiener-Askey polynomial chaos for stochastic differential equations", *SIAM Journal of Scientific Computing*, 24(2), 619-44.

List of Figures

Figure 1: (a) Schematic diagram of base-isolated SDOF system, (b) equivalent linear elastic-viscous damping model of isolator, (c) bi-linear hysteretic model of isolator, and (d) schematic diagram of five-story base-isolated building (MDOF system).

Figure 2: (a) Full tensor product space for a 2D problem ($N = 2$), and (b) corresponding sparse grid ($N = 2$ and κ-$N = 4$).

Figure 3: Flowchart showing steps followed in quantifying effects of uncertainties in the

List of Tables

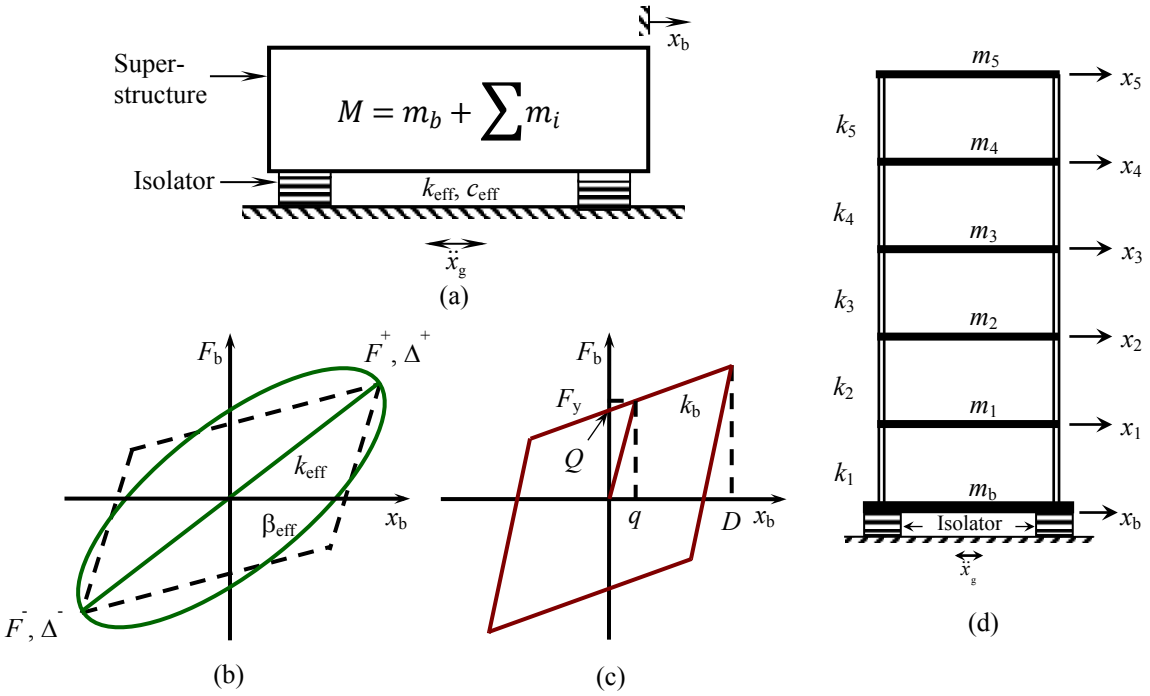

Figure 1: (a) Schematic diagram of base-isolated SDOF system, (b) equivalent linear elastic-viscous damping model of isolator, (c) bi-linear hysteretic model of isolator, and (d) schematic diagram of five-story base-isolated building (MDOF system).

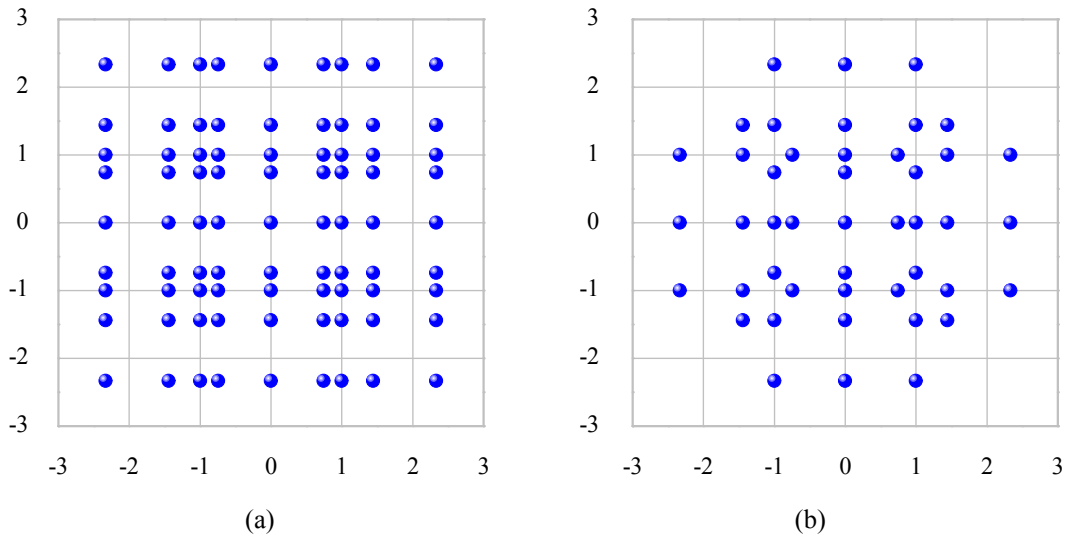

Figure 2: (a) Full tensor product space for a 2D problem ($N = 2$), and (b) corresponding sparse grid ($N = 2$ and κ-$N = 4$).

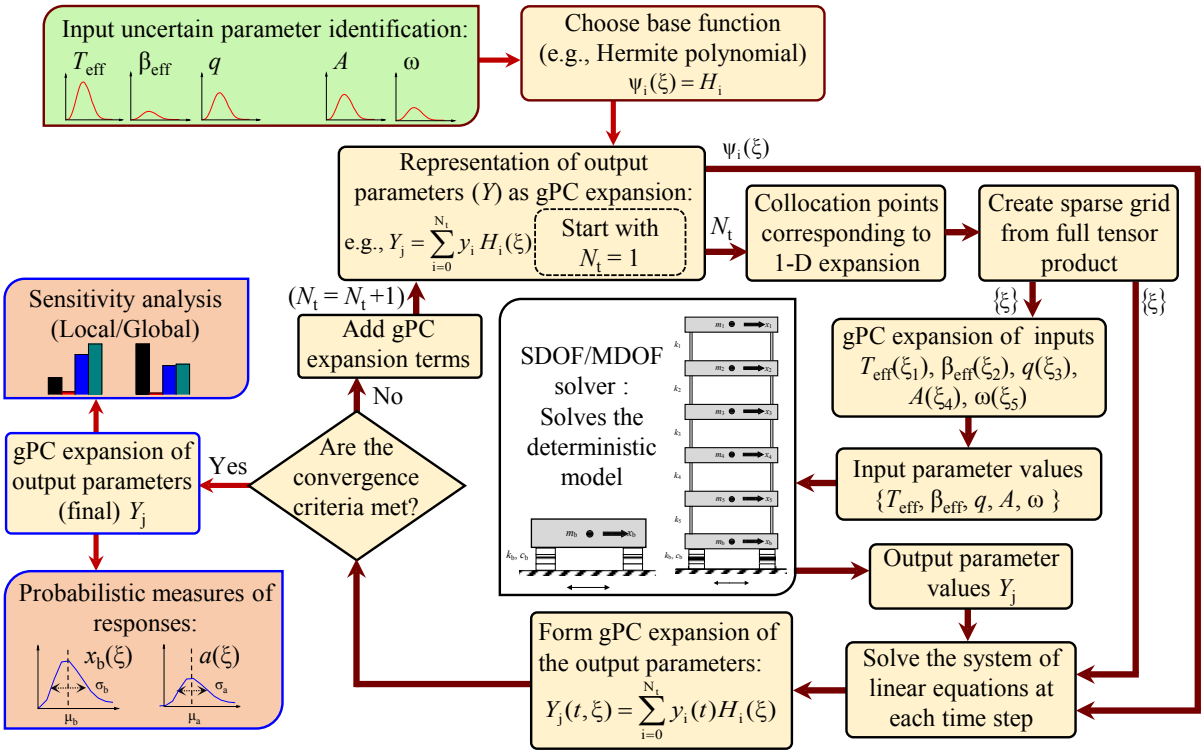

Figure 3: Flowchart showing steps followed in quantifying effects of uncertainties in the dynamic response of the buildings equipped with non-linear base-isolators.

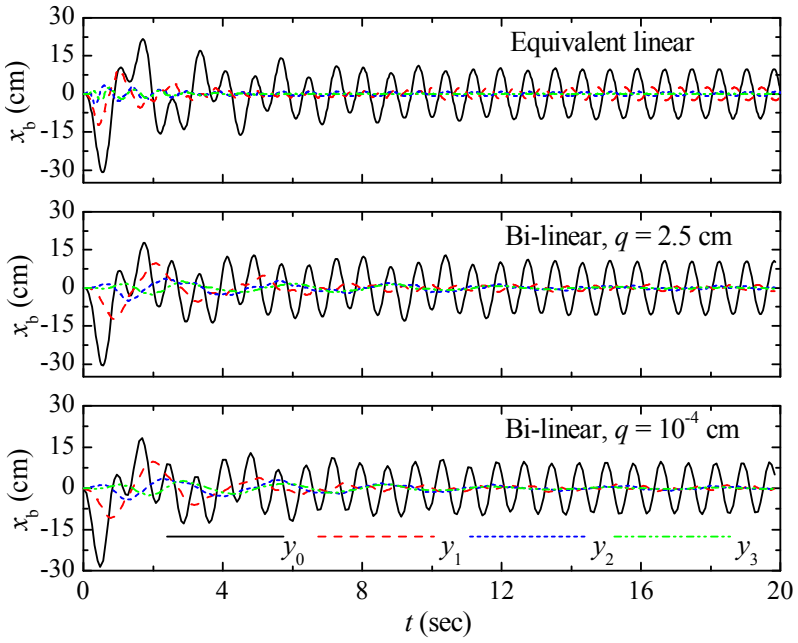

Figure 4: Time histories of 3rd order gPC expansion coefficients for bearing displacement.

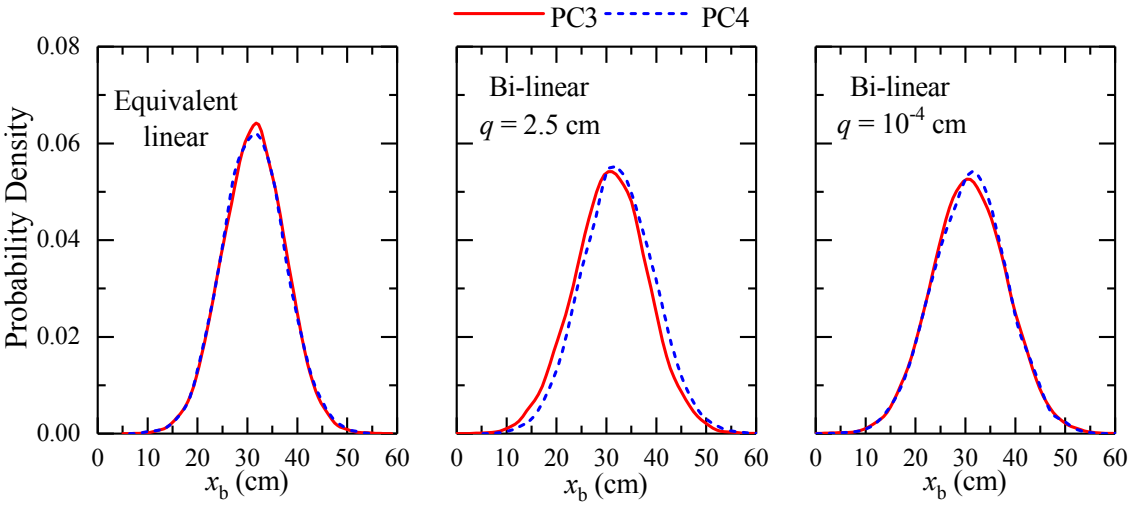

Figure 5: Probability distribution functions of isolation displacement obtained using PC expansion with different orders for base-isolated SDOF.

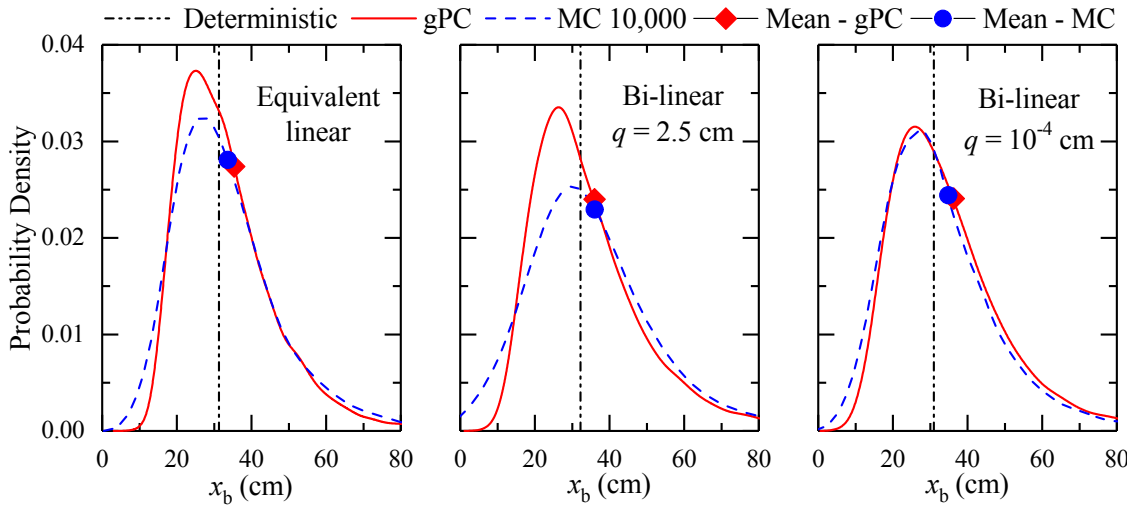

Figure 6: Comparison of probability distribution for peak bearing displacement obtained using gPC expansion technique and MC simulation.

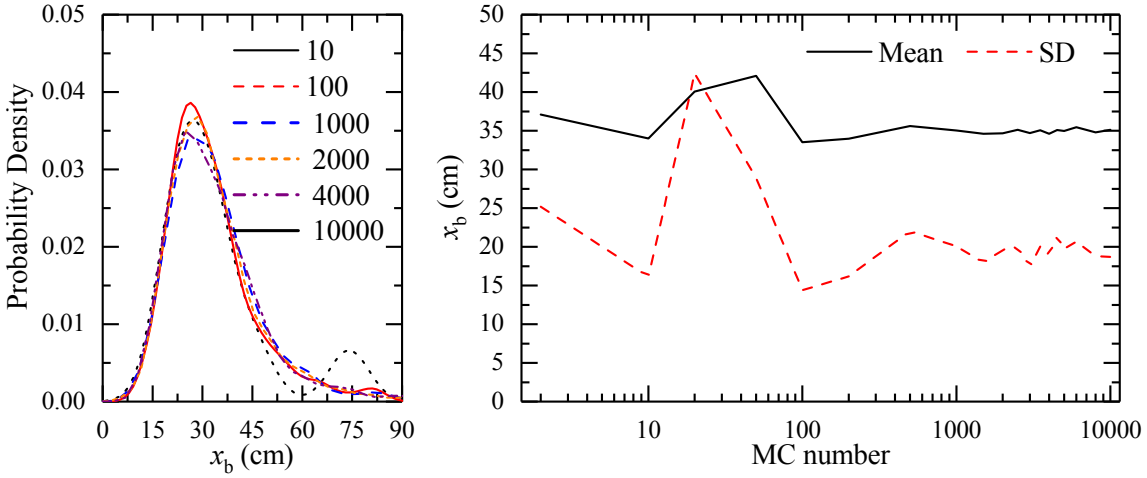

Figure 7: (a) Probability distributions of isolation displacement obtained using the MC simulation with different number of iterations, and (b) mean and standard deviation as a function of the number of Monte Carlo (MC) samples.

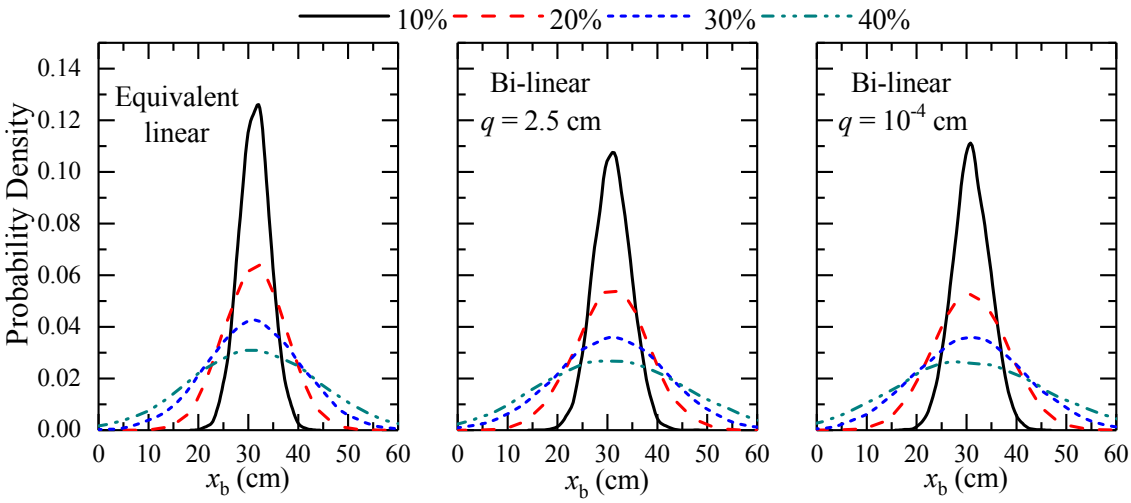

Figure 8: Variation of peak bearing displacement distributions of base-isolated SDOF system with different levels of uncertainties in input parameters.

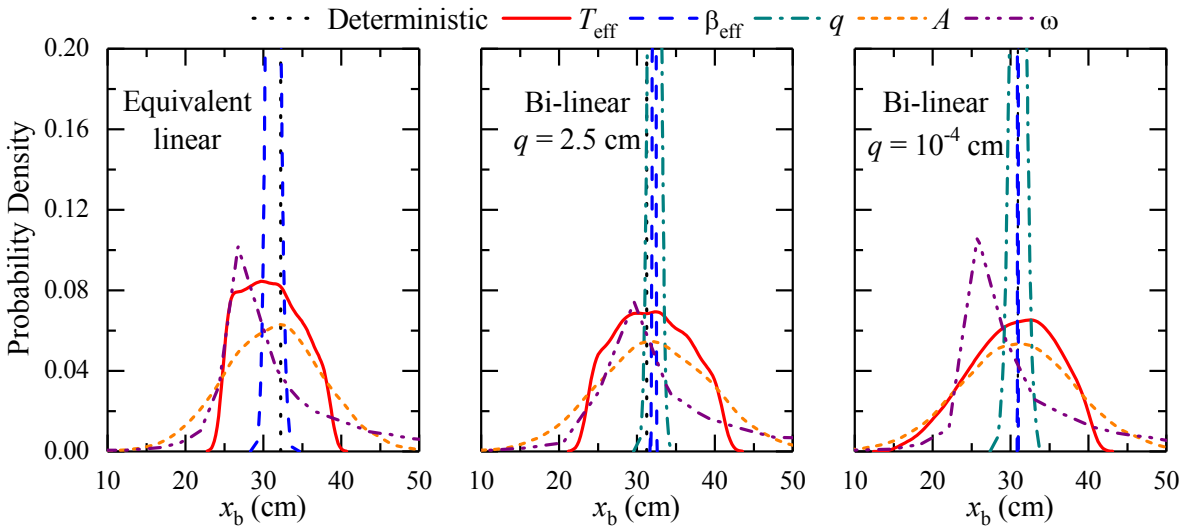

Figure 9: Effect of individual input parameter uncertainties on the distribution of peak bearing displacement of base-isolated SDOF system.

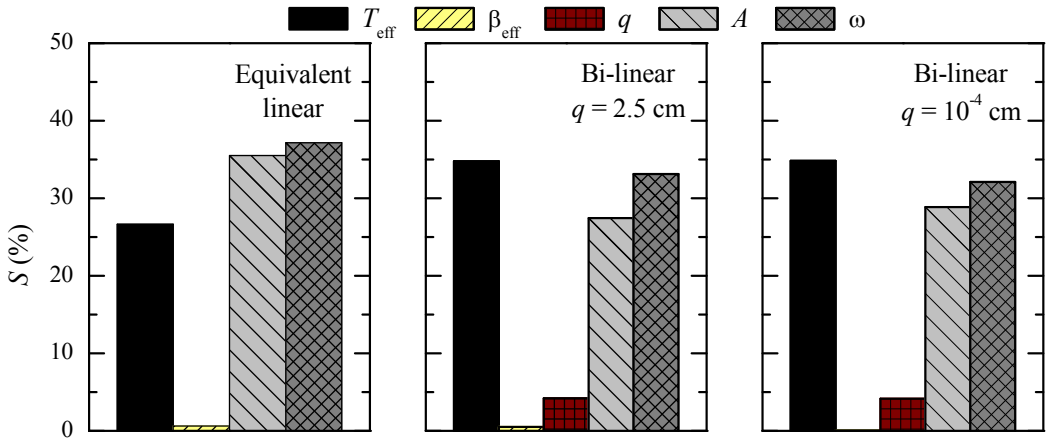

Figure 10: Contribution of each input uncertain parameter towards uncertainty in peak response of base-isolated SDOF system.

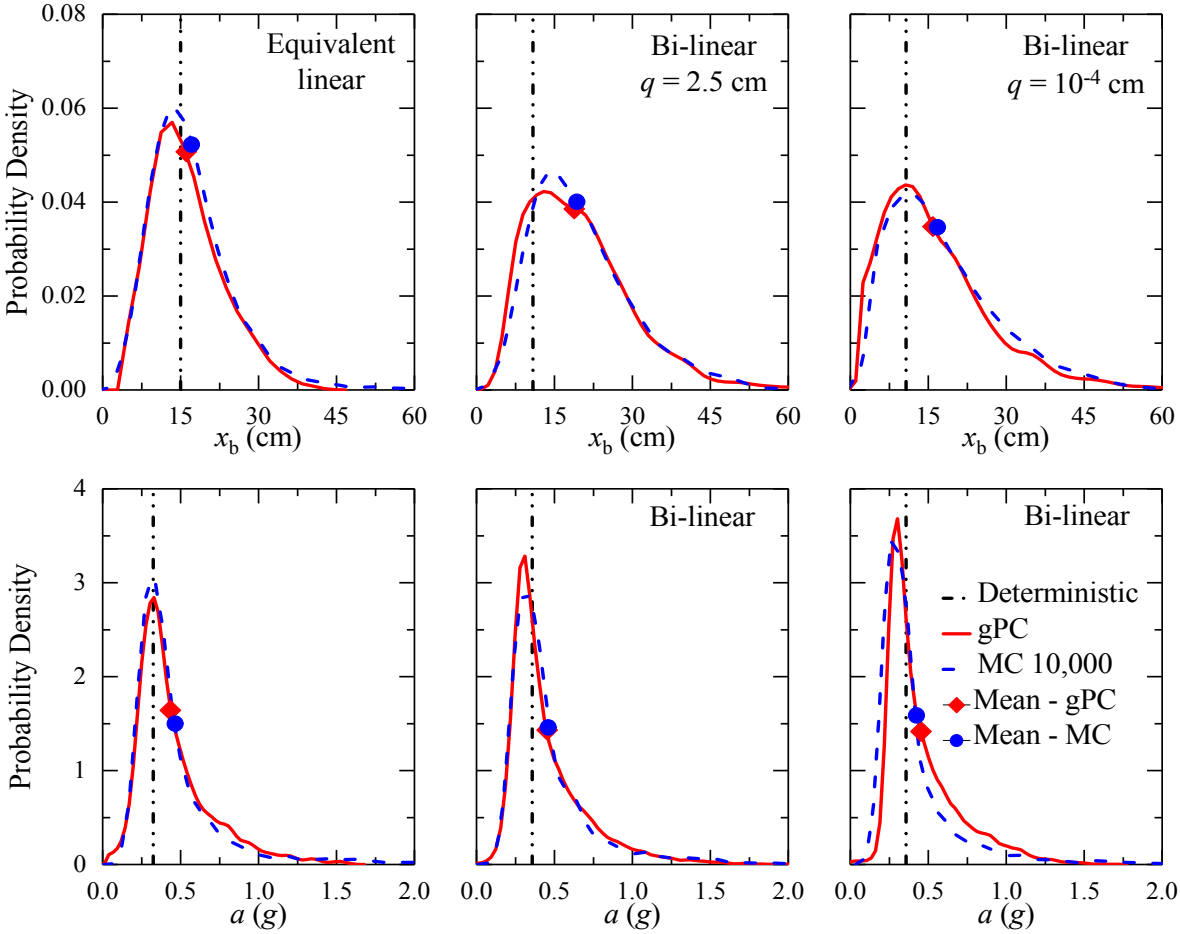

Figure 11: Comparison of probability distributions of dynamic response quantities obtained using gPC expansion and MC simulation for base-isolated MDOF system.

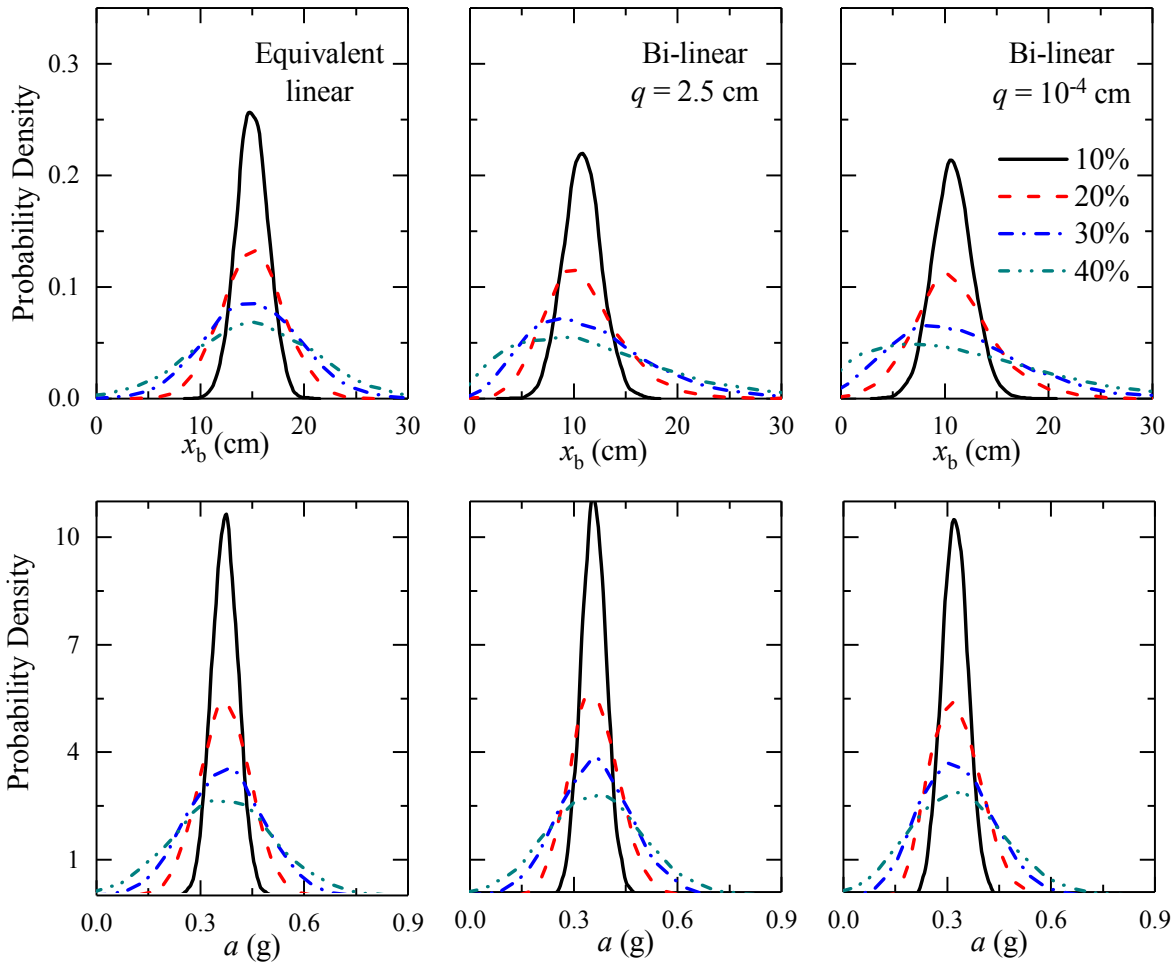

Figure 12: Variation of peak response distributions with different levels of uncertainties in input parameters for base-isolated MDOF system.

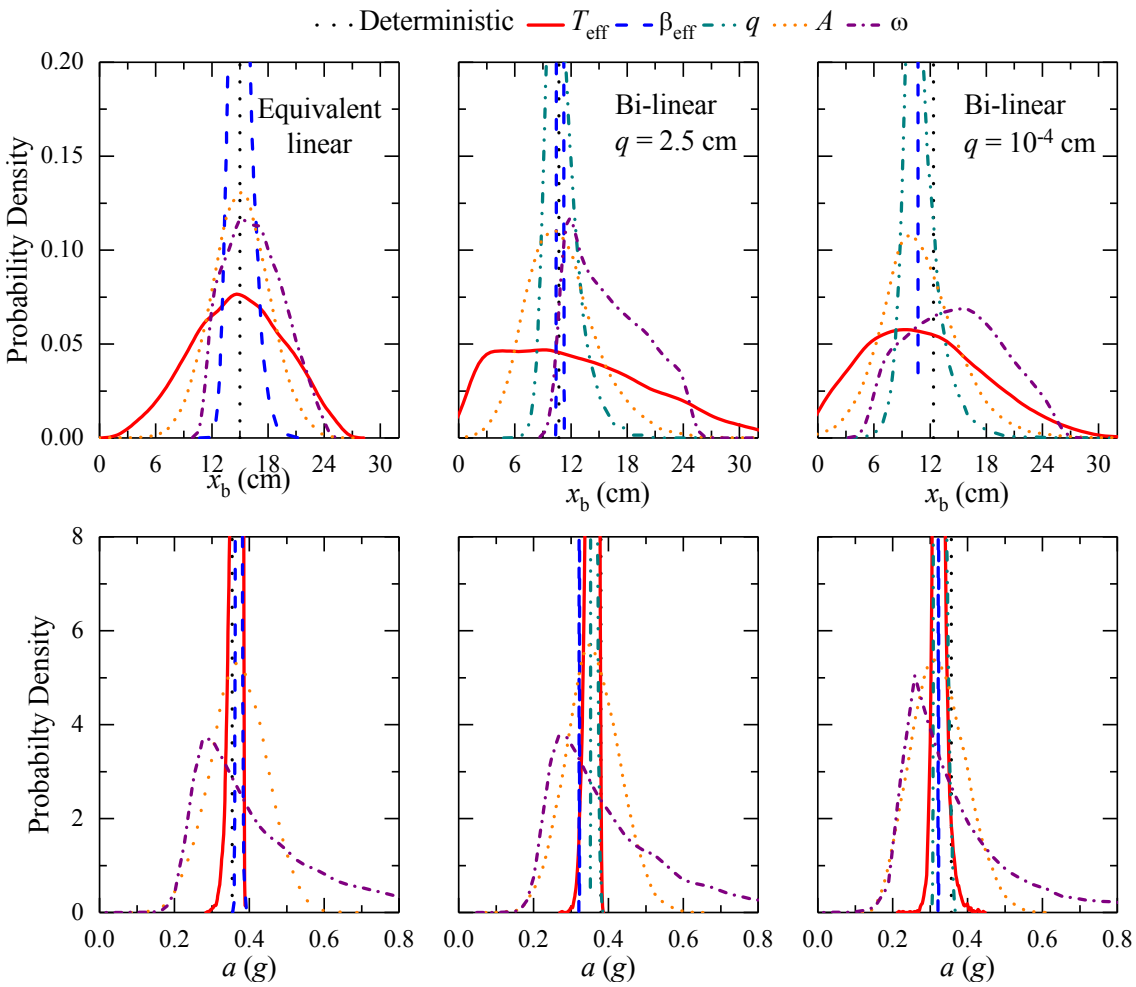

Figure 13: Effect of individual input parameter uncertainties on the peak response distribution of MDOF system.

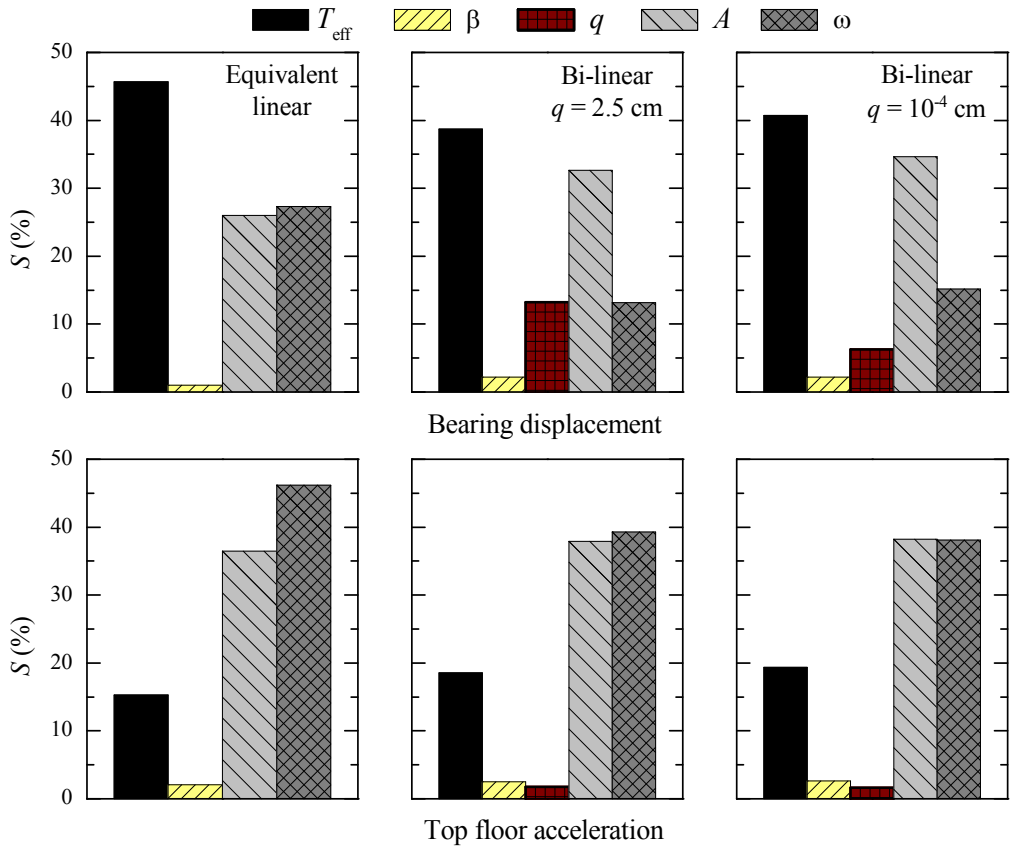

Figure 14: Contribution of individual uncertain input parameter towards uncertainty in peak top floor acceleration and peak bearing displacement of base-isolated MDOF system.

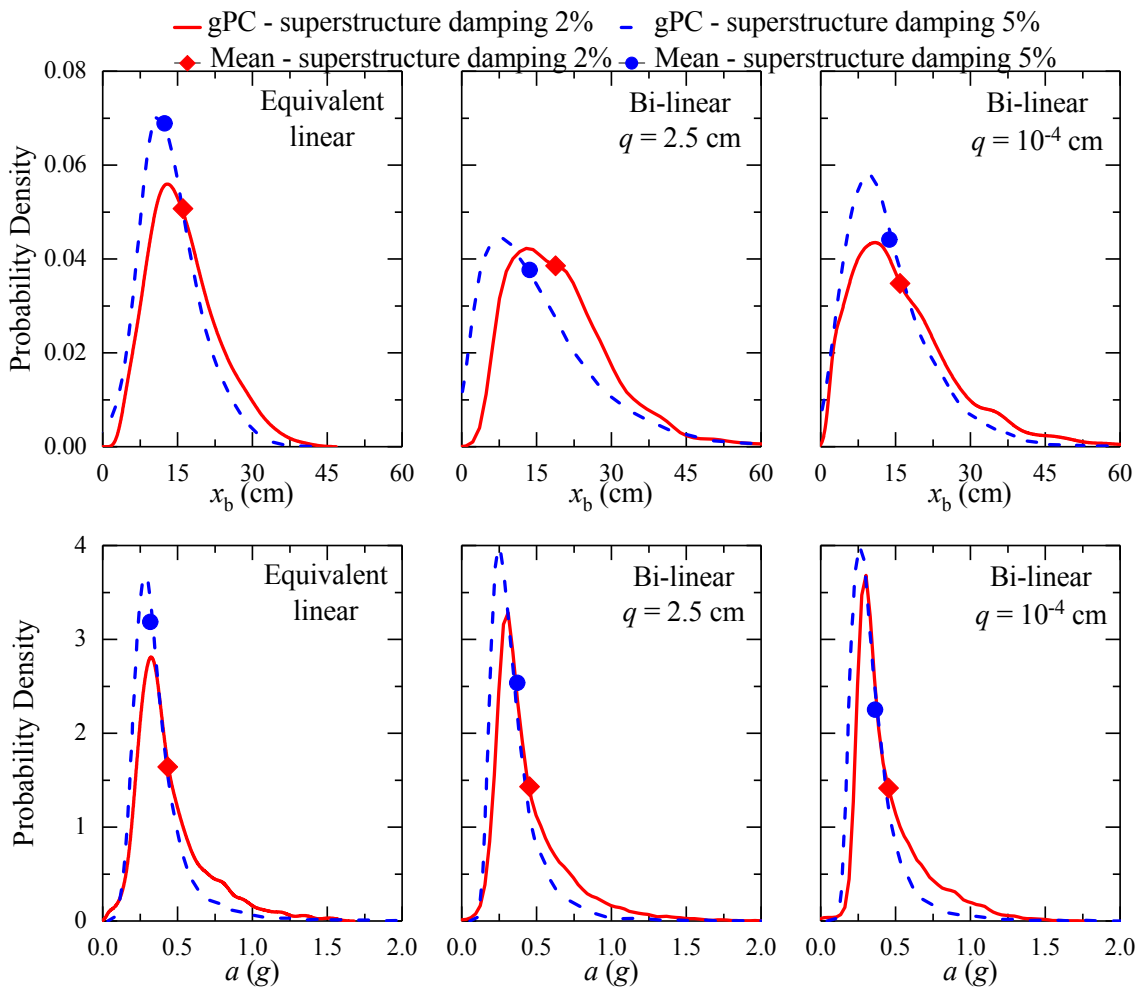

Figure 15: Probability distribution functions of isolation displacement with two superstructure damping values.

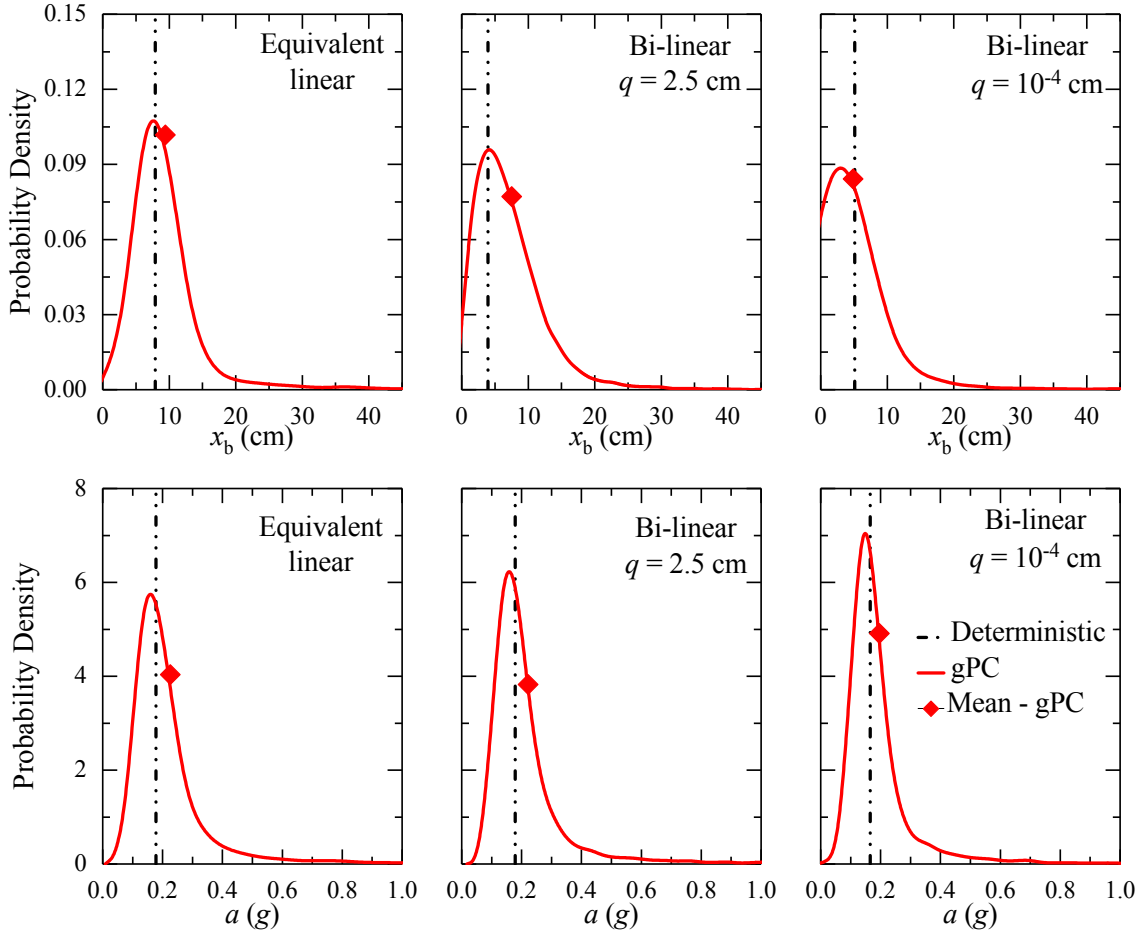

Figure 16: Probability distributions of response quantities obtained using gPC expansion for base-isolated MDOF system subjected to ground excitation - 2.

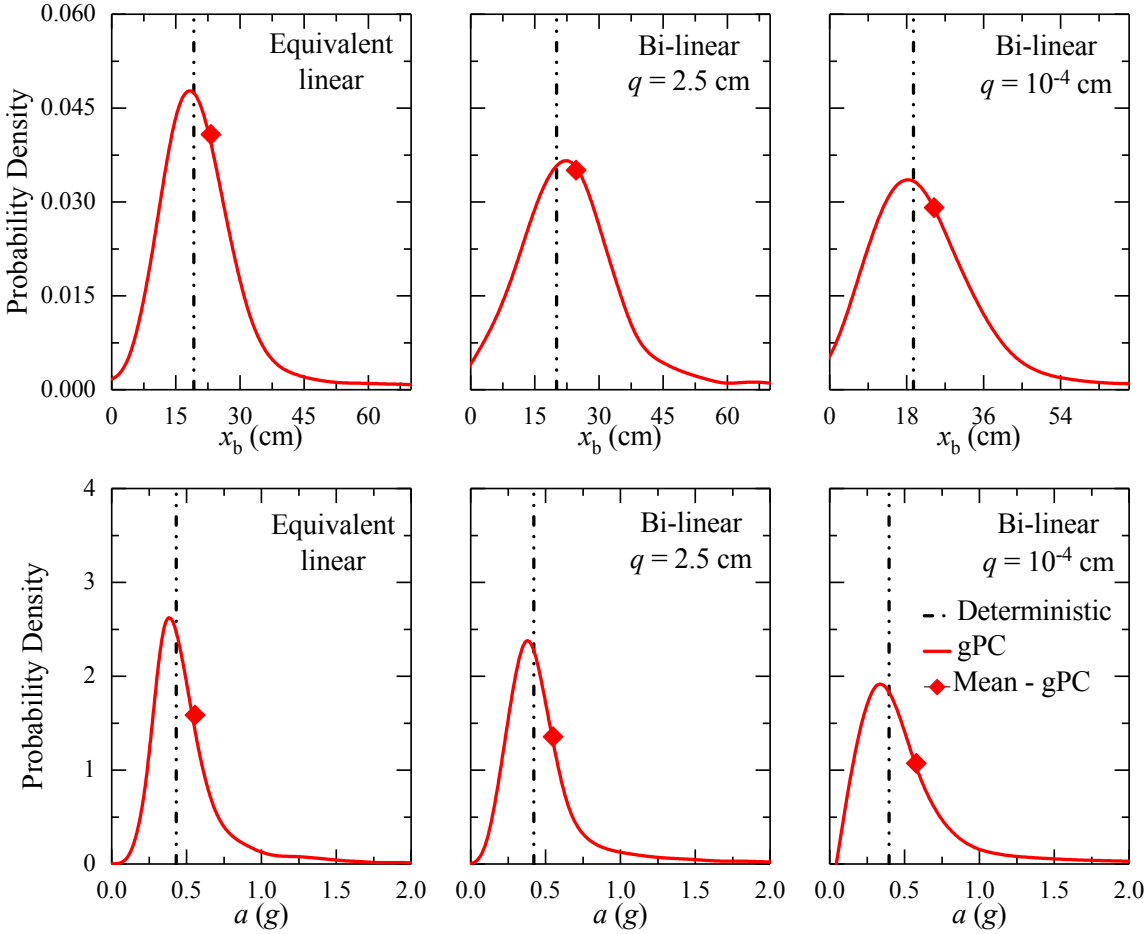

Figure 17: Probability distributions of response quantities obtained using gPC expansion for base-isolated MDOF system subjected to ground excitation - 3.

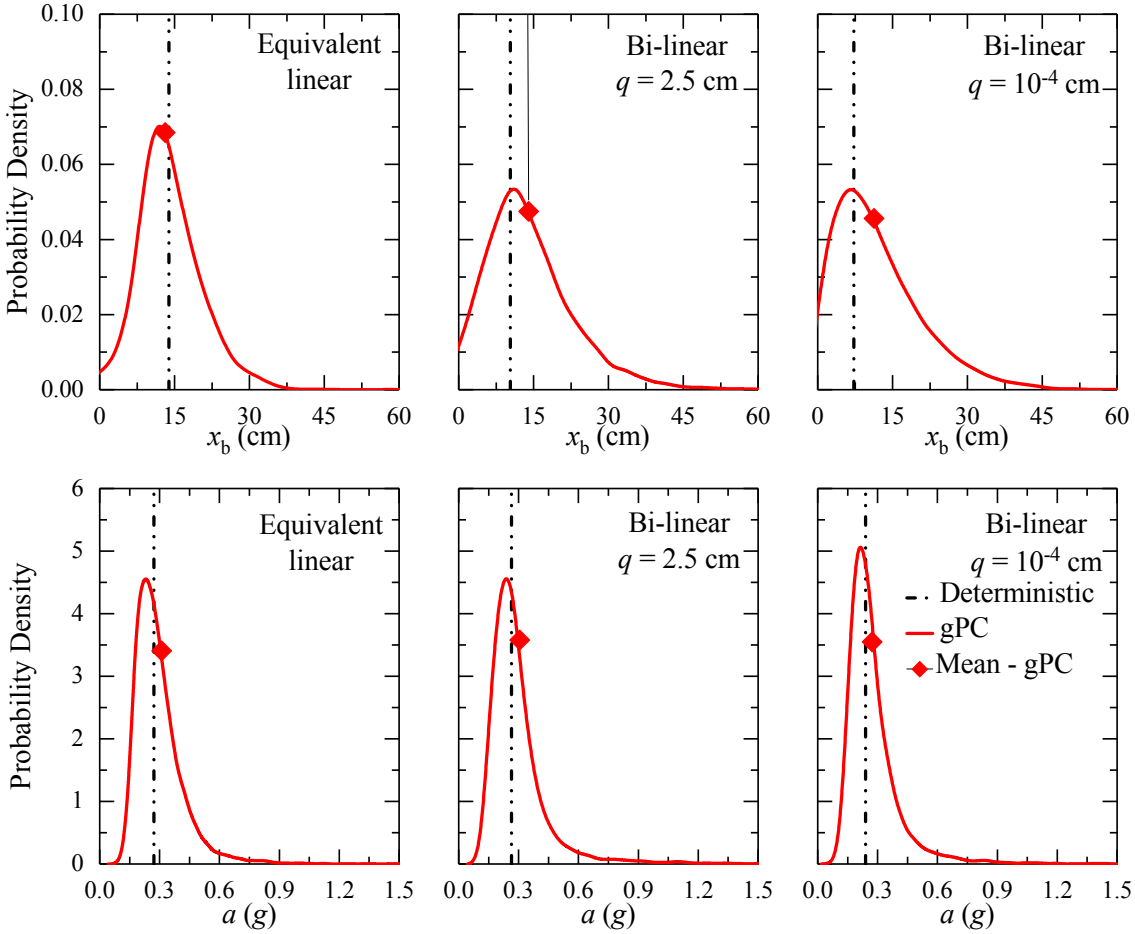

Figure 18: Probability distributions of dynamic response quantities obtained using gPC expansion for base-isolated MDOF system subjected to ground excitation - 4.

Table 1: Mean and standard deviation of input uncertain parameters.

Uncertain parameter	Mean	Standard deviation (SD)
Isolation effective time period (T_{eff}, sec)	2.0	0.40
Isolation damping ratio (β_{eff})	0.1	0.02
Yield displacement of isolator (q, cm)	(i) 2.5 and (ii)10^{-4}	(i) 0.5 and (ii) 0.2×10^{-4}
Amplitude of sinusoidal excitation (m/sec^2) corresponding to ground excitation - 1	5.6	1.12
Frequency of the excitation (rad/sec) corresponding to ground excitation - 1	8.0	1.60

Table 2: Computational time required for gPC expansion technique and MC simulation.

	Computational time (sec)		
	Linear	Bi-linear, q = 2.5 cm	Bi-linear, q = 10^{-4} cm
gPC	158	946	4657
MC 4,000	4880	6304	29952
Ratio for gPC/MC (%)	3.2	15.0	15.54

Table 3: Mean and standard deviation (SD) of bearing displacement for base-isolated SDOF system.

	Bearing displacement (cm)					
	Linear		Bi-linear, q = 2.5 cm		Bi-linear, q = 10^{-4} cm	
	Mean	SD	Mean	SD	Mean	SD
gPC	33.618	14.244	35.989	20.080	36.339	21.190
MC10,000	35.498	16.023	36.044	20.040	34.905	21.786
Deterministic	32.240	-	31.262	-	30.944	-
% difference*	4.27	-	15.12	-	17.43	-

* Percentage difference of mean values obtained by gPC method from deterministic values

Table 4: PC-based Sobol' indices for isolation displacement of base-isolated SDOF system.

	Linear	Bi-linear, q = 2.5 cm	Bi-linear, q = 10^{-4} cm
S_T^T	0.485	0.763	0.762
S_β^T	0.005	0.009	0.008
S_q^T	-	4.21×10^{-4}	4.30×10^{-4}
S_A^T	0.173	0.051	0.052
S_ω^T	0.385	0.383	0.389

Table 5: Mean and standard deviation (SD) of peak response quantities for base-isolated MDOF system.

		Linear		Bi-linear q = 2.5 cm		Bi-linear q = 10^{-4} cm	
Response quantity		Mean	SD	Mean	SD	Mean	SD
Bearing displacement (cm)	gPC	16.064	8.825	18.966	10.727	15.879	11.719
	MC 10,000	17.049	8.781	19.141	10.4805	16.795	12.119
	Deterministic	15.000	-	10.888	-	10.700	-
	% difference*	7.09	-	74.19	-	48.40	-
Top floor acceleration (g)	gPC	0.439	0.257	0.452	0.253	0.453	0.236
	MC 10,000	0.468	0.337	0.464	0.292	0.423	0.323
	Deterministic	0.324	-	0.358	-	0.357	-
	% difference*	35.49		26.26	-	26.89	-

* Percentage difference of mean values obtained by gPC method from deterministic values

Table 6: PC-based Sobol' indices for isolation displacement of base-isolated MDOF system.

	Linear	Bi-linear, q = 2.5 cm	Bi-linear, q = 10^{-4} cm
S_{T}^{T}	0.235	0.720	0.576
S_{β}^{T}	0.016	0.210	0.039
S_{q}^{T}	-	0.002	0.002
S_{A}^{T}	0.151	0.231	0.262
S_{ω}^{T}	0.627	0.406	0.220

Table 7: PC-based Sobol' indices for top floor acceleration of base-isolated MDOF system.

	Linear	Bi-linear, q = 2.5 cm	Bi-linear, q = 10^{-4} cm
S_{T}^{T}	0.042	0.012	0.023
S_{β}^{T}	0.004	0.003	0.007
S_{q}^{T}	-	3.99×10^{-4}	9.26×10^{-4}
S_{A}^{T}	0.108	0.113	0.147
S_{ω}^{T}	0.902	0.895	0.880

Table 8: Mean and standard deviation of amplitude and frequencies corresponding to recorded ground excitations.

Excitation No.	Reference earthquake	Uncertain parameter	Mean	Standard deviation (SD)
Ground excitation - 2	1940, Imperial valley (00 component), recorded at El Centro	Amplitude of sinusoidal excitation (m/sec^2)	3.3	0.66
		Frequency of the excitation (rad/sec)	9.2	1.84
Ground excitation - 3	1995, Kobe (NS component), recorded at JMA	Amplitude of sinusoidal excitation (m/sec^2)	8	1.6
		Frequency of the excitation (rad/sec)	9.2	1.84
Ground excitation - 4	1989, Loma Prieta (90 component), recorded at Los Gatos Presentation Centre	Amplitude of sinusoidal excitation (m/sec^2)	5.8	1.16
		Frequency of the excitation (rad/sec)	10.2	2.04

Table 9: Mean and standard deviation (SD) of peak dynamic response quantities for base-isolated MDOF system for ground excitations 2, 3, and 4.

		Linear			Bi-linear q = 2.5 cm			Bi-linear $q = 10^{-4}$ cm		
Response quantity	Excitation No.	Deterministic	Mean	SD	Deterministic	Mean	SD	Deterministic	Mean	SD
Bearing displacement (cm)	Ground excitation - 2	7.909	9.372	8.620	3.952	7.125	5.672	5.106	4.805	7.057
	Ground excitation - 3	19.18	23.15	22.48	20.06	24.89	18.18	19.58	24.14	22.73
	Ground excitation - 4	13.87	12.79	10.64	10.35	14.08	9.08	7.298	11.86	8.95
Top floor acceleration (g)	Ground excitation - 2	0.178	0.221	0.181	0.179	0.218	0.174	0.165	0.195	0.152
	Ground excitation - 3	0.431	0.544	0.459	0.421	0.552	0.606	0.396	0.573	0.771
	Ground excitation - 4	0.272	0.295	0.123	0.264	0.298	0.173	0.240	0.277	0.147

Table 10: PC-based Sobol' indices of peak dynamic response quantities for base-isolated MDOF system for ground excitations 2,3, and 4.

Response quantity	Sobol' indices	Linear			Bi-linear q = 2.5 cm			Bi-linear $q = 10^{-4}$ cm		
		Ground excitation no.			Ground excitation no.			Ground excitation no.		
		2	3	4	2	3	4	2	3	4
Bearing displacement (cm)	S_T^T	0.080	0.080	0.473	0.432	0.242	0.651	0.234	0.153	0.485
	S_β^T	0.004	0.004	0.042	0.052	0.008	0.049	0.042	0.013	0.079
	S_q^T	-	-	-	0.011	0.0008	0.005	0.0008	0.0002	0.0002
	S_A^T	0.064	0.064	0.169	0.1915	0.153	0.240	0.1451	0.105	0.256
	S_ω^T	0.860	0.861	0.406	.372	0.617	0.174	0.606	0.749	0.269
Top floor acceleration (g)	S_T^T	0.002	0.002	0.007	0.005	0.0007	0.006	0.015	0.0005	0.012
	S_β^T	3×10^{-4}	0.0003	0.0009	0.0002	0.001	0.0007	0.002	0.0008	0.006
	S_q^T	-	-	-	0.0006	0.0000	0.0002	0.0000	0.0000	0.0000
	S_A^T	0.070	0.069	0.234	0.071	0.050	0.132	0.057	0.032	0.166
	S_ω^T	0.934	0.934	0.778	0.935	0.961	0.875	0.934	0.971	0.838